

RECENT RESULTS FROM LATTICE QCD



WWND2016

Claudia Ratti
University of Houston (USA)

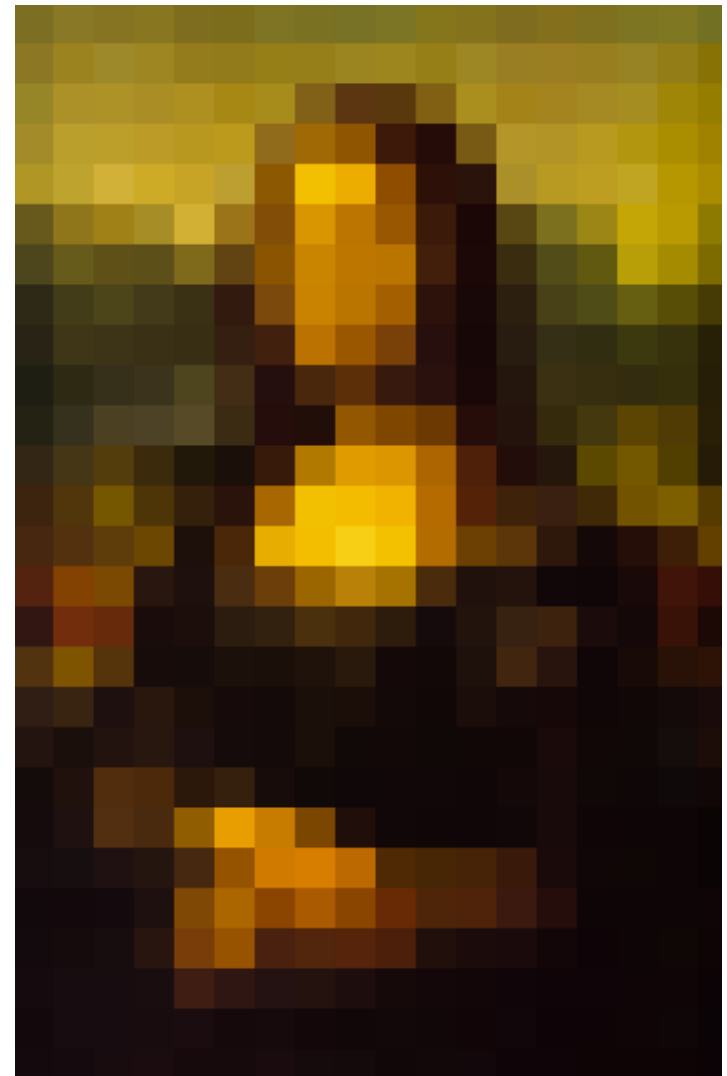
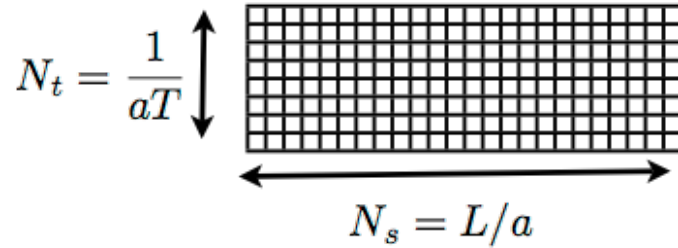


Lattice QCD

- Best first principle-tool to extract predictions for the theory of strong interactions in the non-perturbative regime
- Uncertainties:
 - ▣ Statistical: finite sample, error $\sim 1/\sqrt{\text{sample size}}$
 - ▣ Systematic: finite box size, unphysical quark masses
- Given enough computer power, uncertainties can be kept under control
- Results from different groups, adopting different discretizations, converge to consistent results
- Unprecedented level of accuracy in lattice data

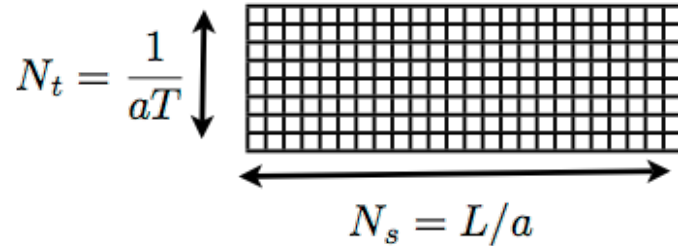
Importance of continuum limit

- Lattice action: parametrization used to discretize the Lagrangian of QCD on a space-time grid

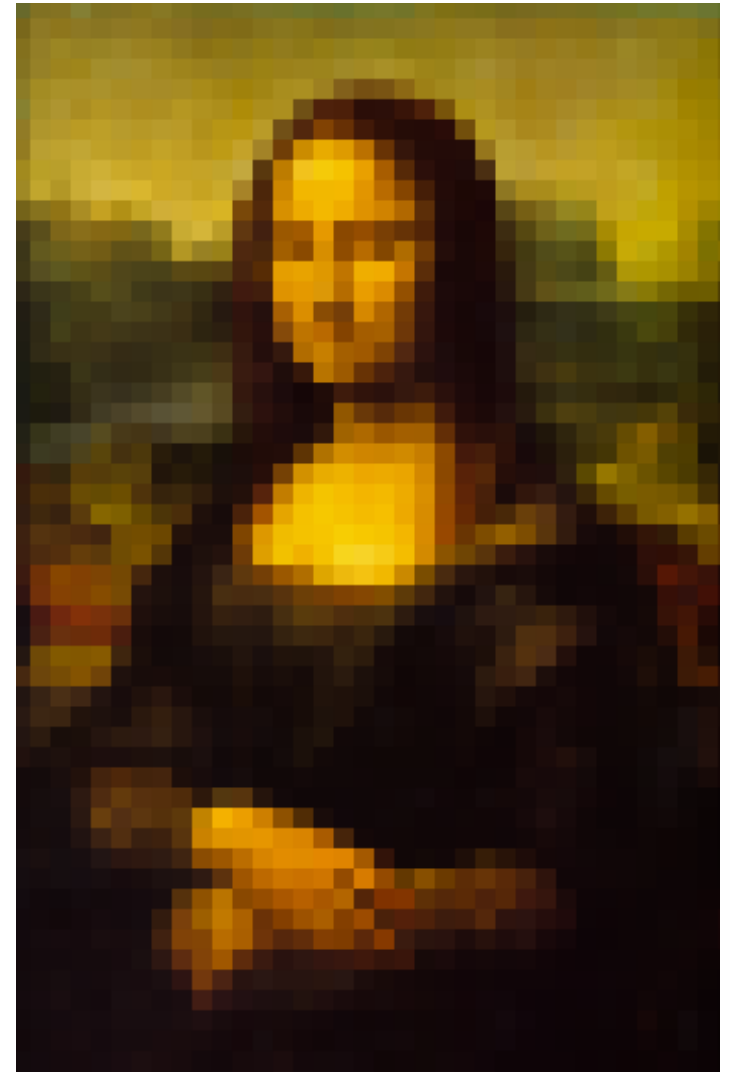


Importance of continuum limit

- Lattice action: parametrization used to discretize the Lagrangian of QCD on a space-time grid

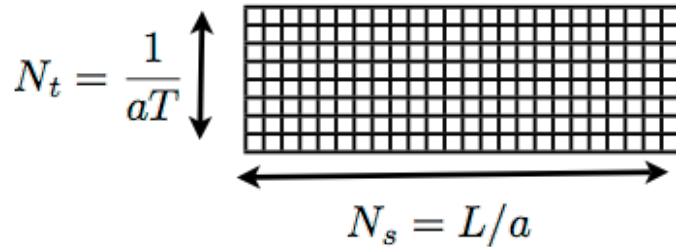


- Repeat the simulations on finer lattices (smaller $a \leftrightarrow$ larger N_t)

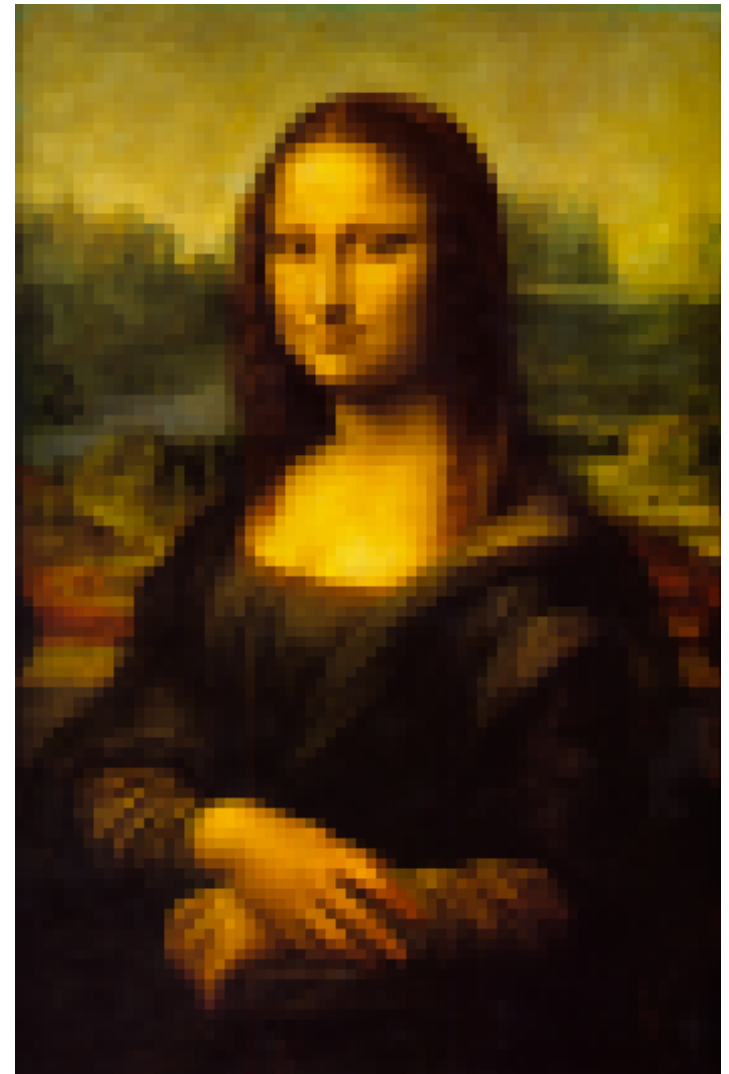
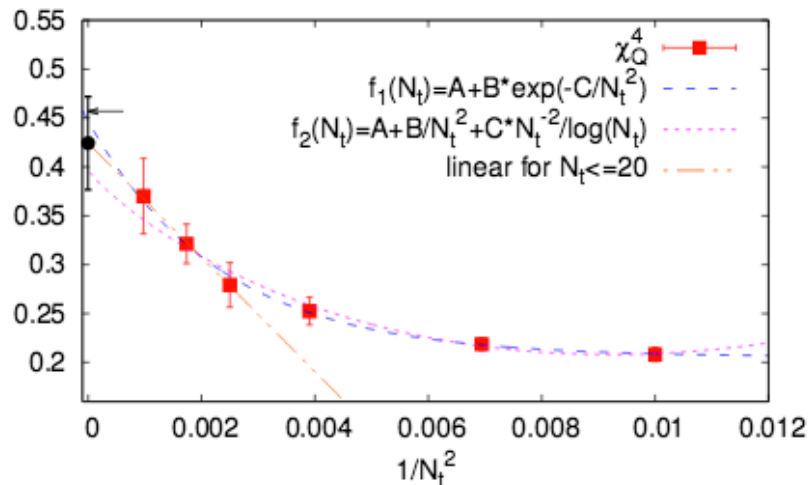


Importance of continuum limit

- Lattice action: parametrization used to discretize the Lagrangian of QCD on a space-time grid

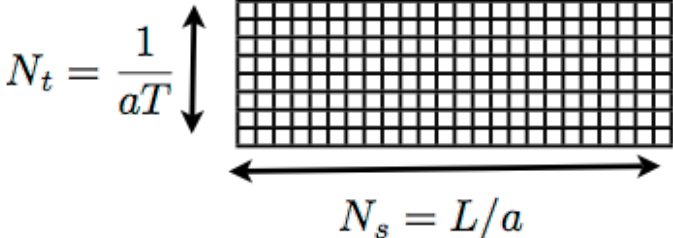


- Repeat the simulations on finer lattices (smaller $a \leftrightarrow$ larger N_t)

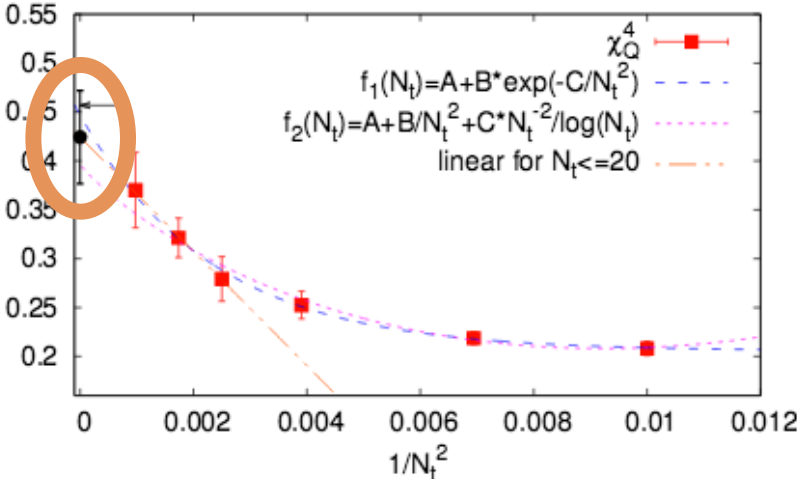


Importance of continuum limit

- Lattice action: parametrization used to discretize the Lagrangian of QCD on a space-time grid

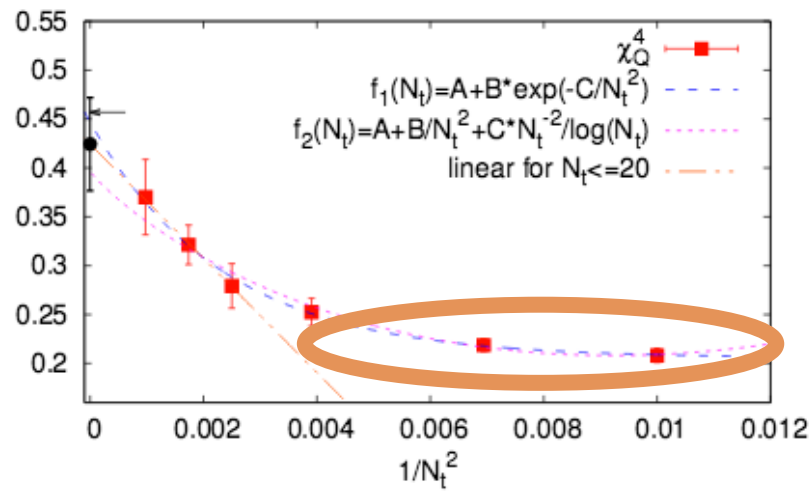


- Repeat the simulations on finer lattices (smaller $a \leftrightarrow$ larger N_t)



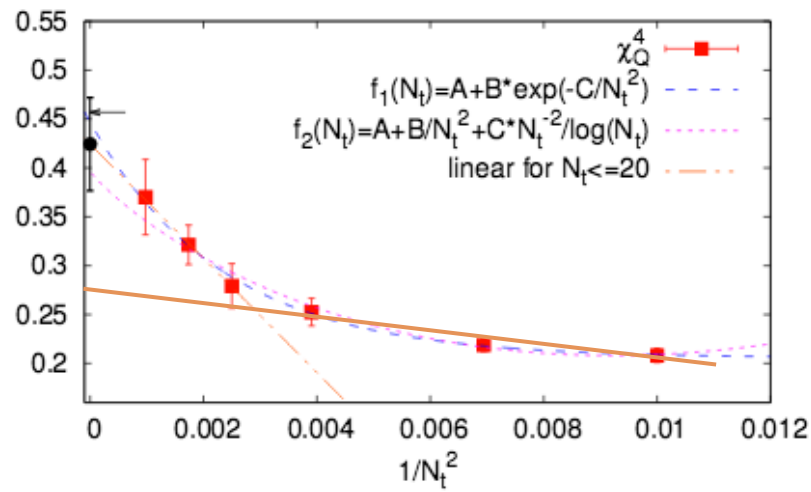
Importance of continuum limit

- Observables are affected by discretization effects differently



Importance of continuum limit

- Observables are affected by discretization effects differently
- In quantitative predictions, finite- N_t results can lead to misleading information



Importance of continuum limit

- Observables are affected by discretization effects differently
- In quantitative predictions, finite- N_t results can lead to misleading information
- **Message:** continuum extrapolated data always preferable



Low temperature phase: HRG model

Dashen, Ma, Bernstein; Prakash, Venugopalan, Karsch, Tawfik, Redlich

- **Interacting** hadronic matter in the **ground state** can be well approximated by a **non-interacting** resonance gas
- The pressure can be written as:

$$p^{HRG}/T^4 = \frac{1}{VT^3} \sum_{i \in \text{mesons}} \ln \mathcal{Z}_{m_i}^M(T, V, \mu_{X^a}) + \frac{1}{VT^3} \sum_{i \in \text{baryons}} \ln \mathcal{Z}_{m_i}^B(T, V, \mu_{X^a})$$

where

$$\ln \mathcal{Z}_{m_i}^{M/B} = \mp \frac{V d_i}{2\pi^2} \int_0^\infty dk k^2 \ln(1 \mp z_i e^{-\varepsilon_i/T}) ,$$

with energies $\varepsilon_i = \sqrt{k^2 + m_i^2}$, degeneracy factors d_i and fugacities

$$z_i = \exp \left(\left(\sum_a X_i^a \mu_{X^a} \right) / T \right) .$$

X^a : all possible conserved charges, including the baryon number B , electric charge Q , strangeness S .

- Up to which temperature do we expect agreement with the lattice data?

High temperature limit

- QCD thermodynamics approaches that of a non-interacting, massless quark-gluon gas:

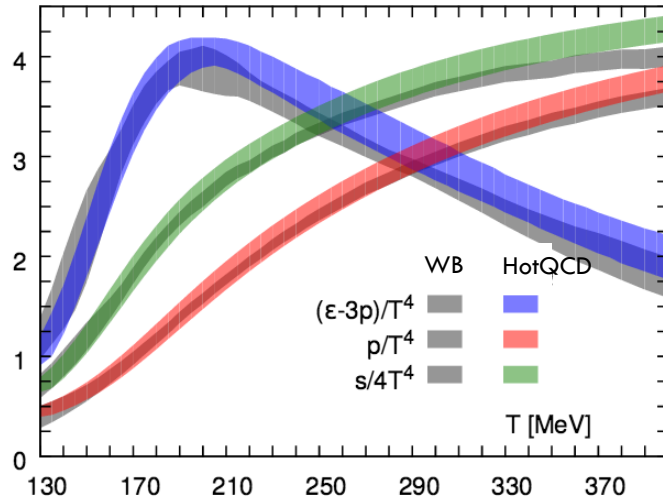
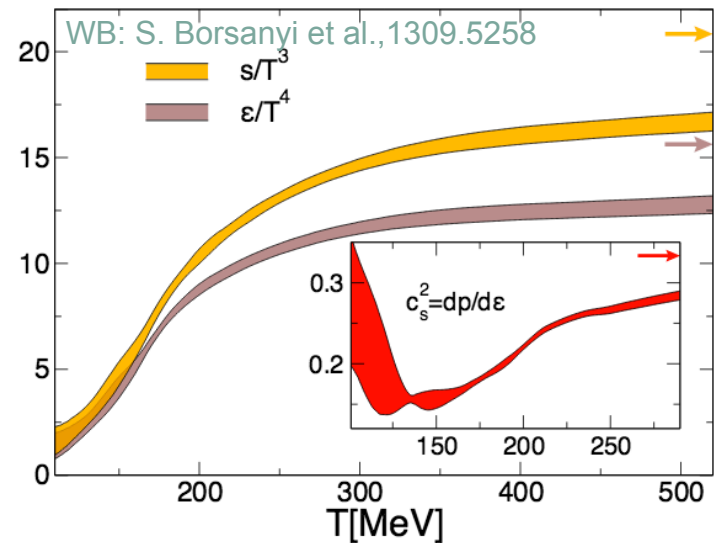
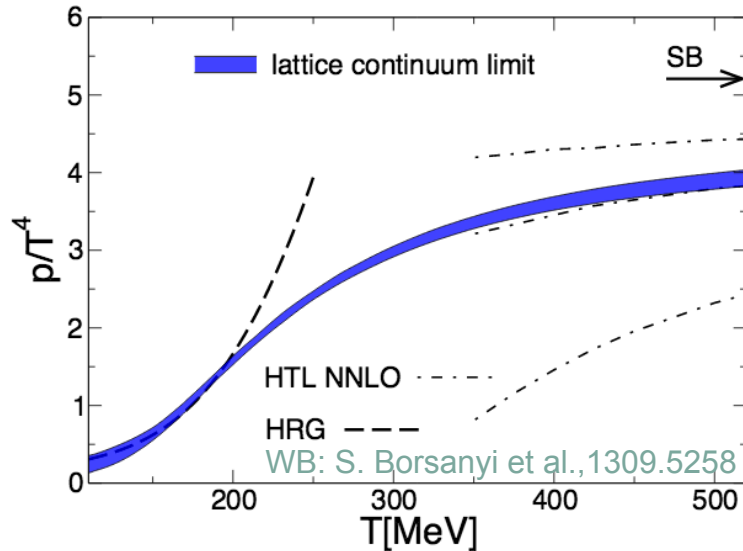
$$\left(\frac{P}{T^4}\right)_{\text{ideal}} = \frac{8\pi^2}{45} + \sum_{f=u,d,s} \left[\frac{7\pi^2}{60} + \frac{1}{2} \left(\frac{\mu_f}{T}\right)^2 + \frac{1}{4\pi^2} \left(\frac{\mu_f}{T}\right)^4 \right]$$

- We can switch on the interaction and systematically expand the observables in series of the coupling g
- Resummation of diagrams (HTL) or dimensional reduction are needed, to improve convergence

Braaten, Pisarski (1990); Haque et al. (2014); Hietanen et al (2009)

- At what temperature does perturbation theory break down?

QCD Equation of state at $\mu_B=0$



- EoS available in the **continuum limit**, with realistic quark masses
- **Agreement** between **stout** and **HISQ** action for all quantities

WB: S. Borsanyi et al., 1309.5258, PLB (2014)
 HotQCD: A. Bazavov et al., 1407.6387, PRD (2014)

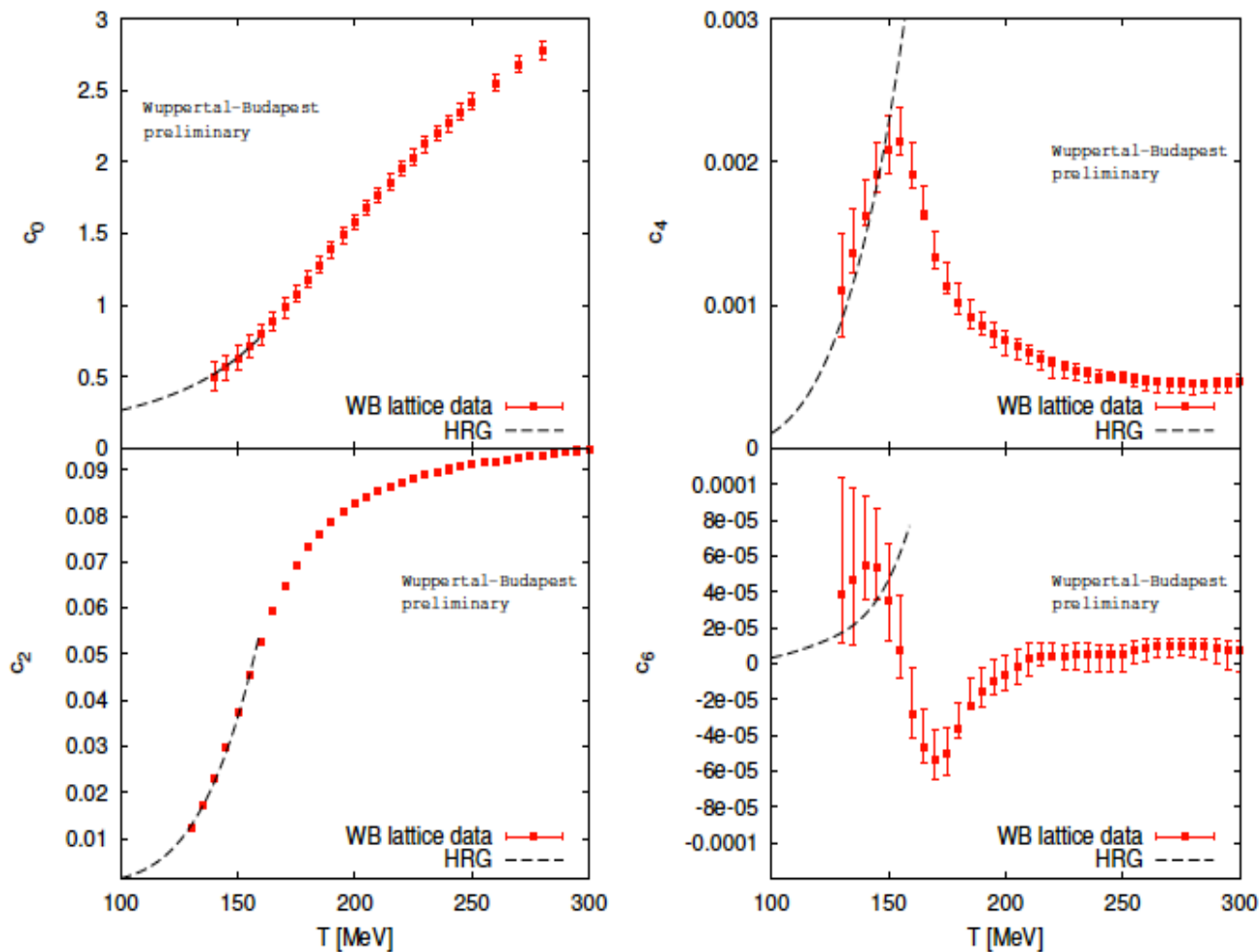
Sign problem

- The QCD path integral is computed by Monte Carlo algorithms which samples field configurations with a weight proportional to the exponential of the action

$$Z(\mu_B, T) = \text{Tr} \left(e^{-\frac{H_{\text{QCD}} - \mu_B N_B}{T}} \right) = \int \mathcal{D}U e^{-S_G[U]} \det M[U, \mu_B]$$

- $\det M[\mu_B]$ complex \rightarrow Monte Carlo simulations are not feasible
- We can rely on a few approximate methods, viable for small μ_B/T :
 - Taylor expansion of physical quantities around $\mu=0$ (Bielefeld-Swansea collaboration 2002; R. Gai, S. Gupta 2003)
 - Reweighting (complex phase moved from the measure to observables) (Barbour et al. 1998; Z. Fodor and S. Katz, 2002)
 - Simulations at imaginary chemical potentials (plus analytic continuation) (Alford, Kapustin, Wilczek, 1999; de Forcrand, Philipsen, 2002; D'Elia, Lombardo 2003)

Equation of state at $\mu_B > 0$



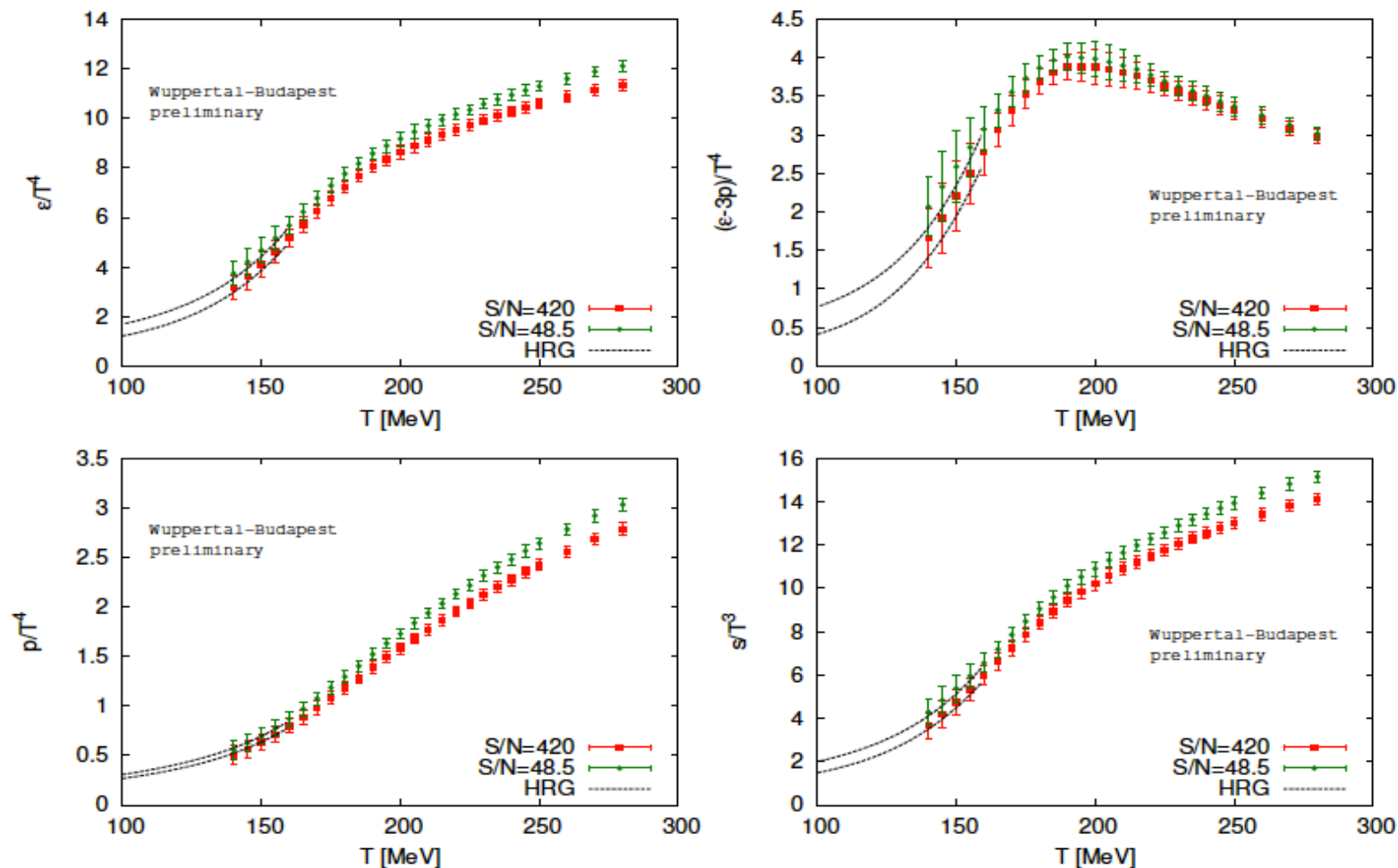
- Expand the pressure in powers of μ_B

$$\frac{p(\mu_B)}{T^4} = c_0 + c_2 \left(\frac{\mu_B}{T}\right)^2 + c_4 \left(\frac{\mu_B}{T}\right)^4 + c_6 \left(\frac{\mu_B}{T}\right)^6 + \mathcal{O}(\mu_B^8)$$

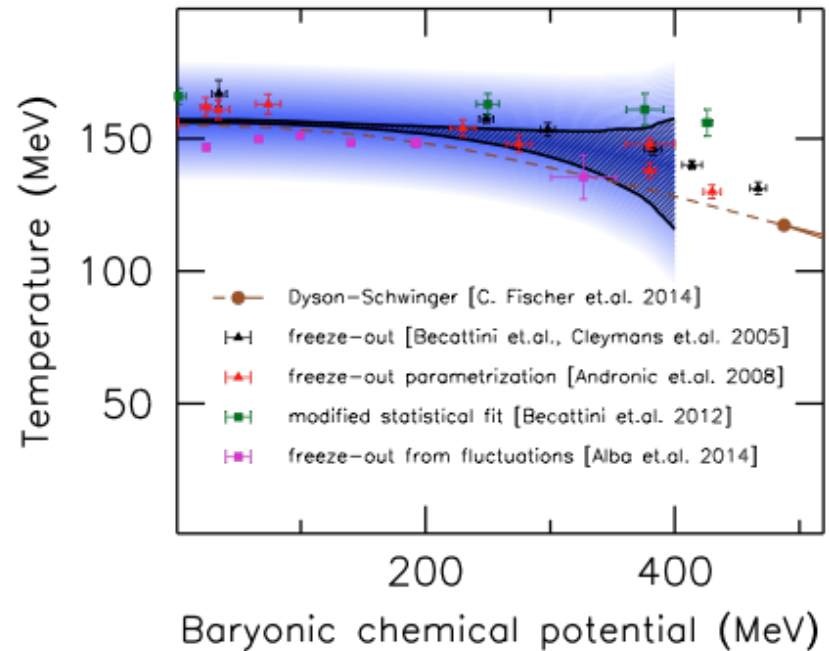
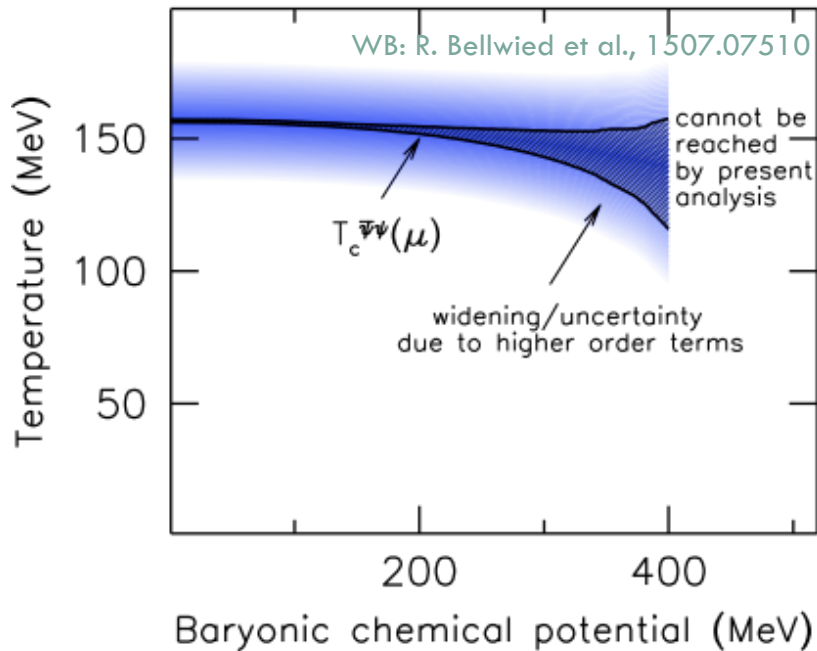
- Continuum extrapolated results for c_2 , c_4 , c_6 at the physical mass

Equation of state at $\mu_B > 0$

- Calculate the EoS along the constant S/N trajectories



QCD phase diagram



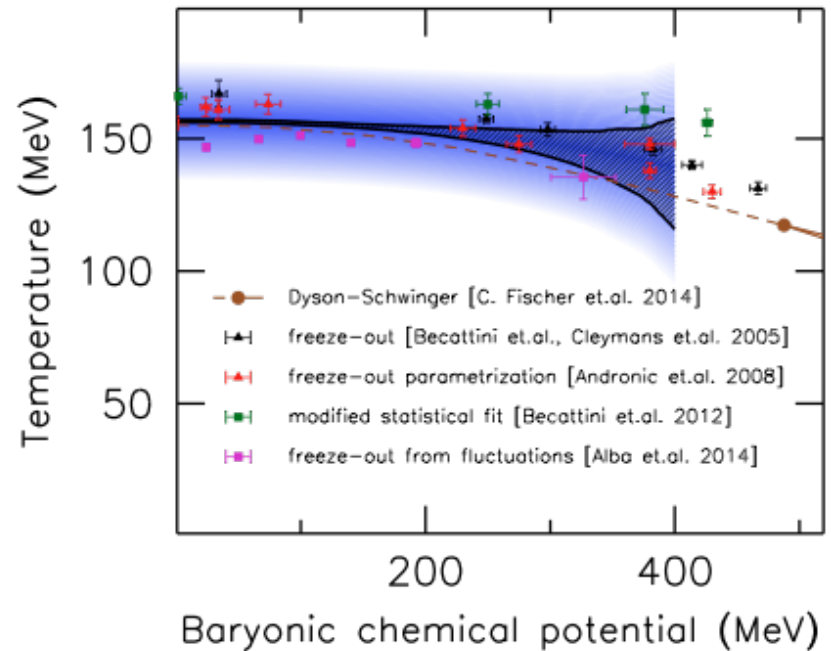
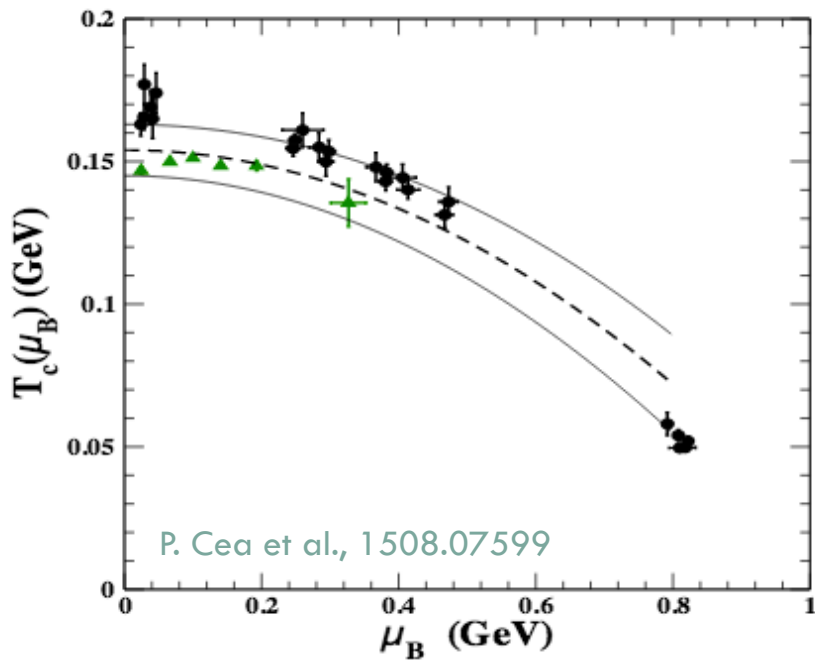
Curvature κ defined as:

$$\frac{T_c(\mu_B)}{T_c(\mu = 0)} = 1 - \kappa \left(\frac{\mu_B}{T_c(\mu_B)} \right)^2 + \lambda \left(\frac{\mu_B}{T_c(\mu_B)} \right)^4 \dots$$

Recent results:

$$\kappa = 0.0149 \pm 0.0021$$

QCD phase diagram



Curvature κ defined as:

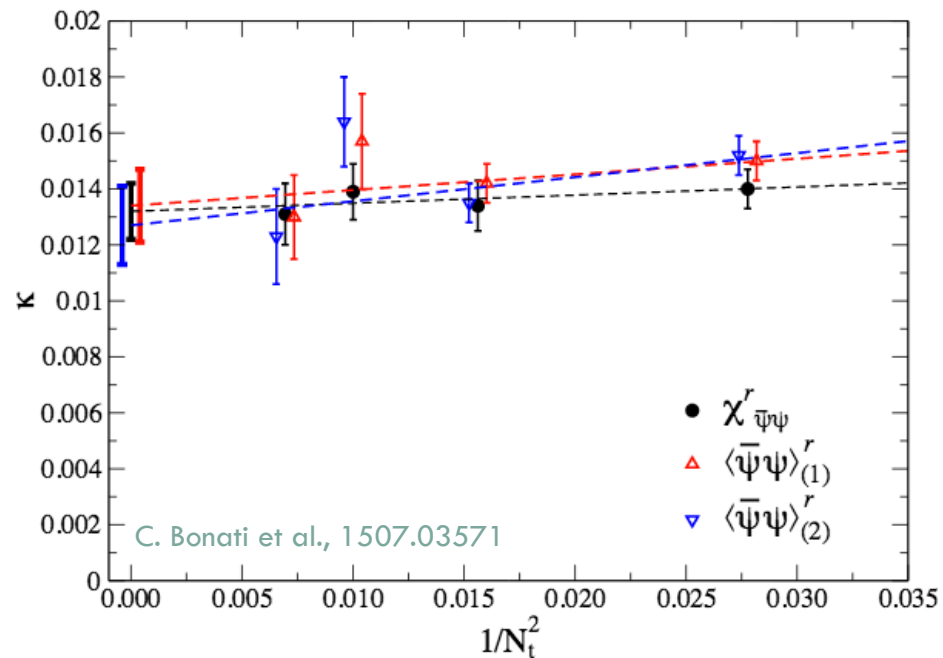
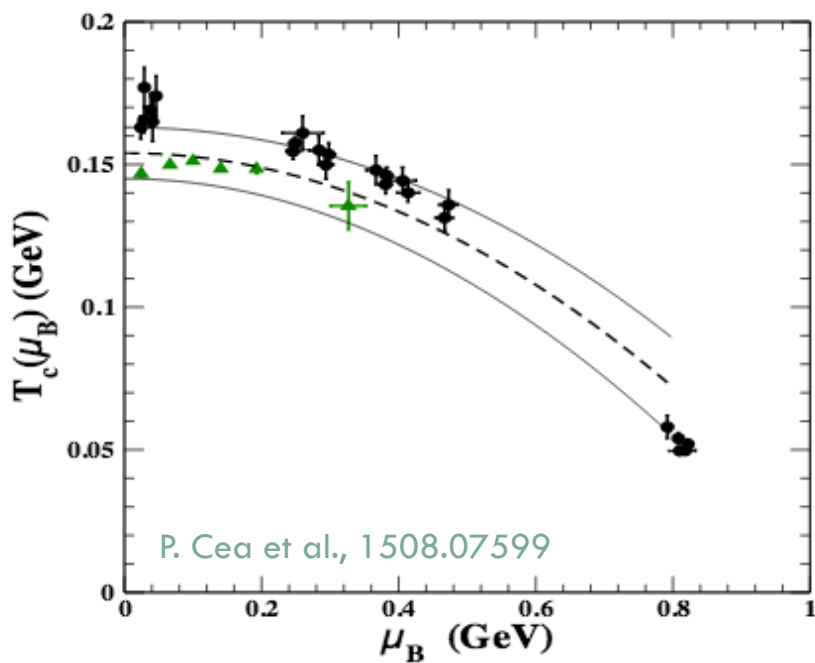
$$\frac{T_c(\mu_B)}{T_c(\mu = 0)} = 1 - \kappa \left(\frac{\mu_B}{T_c(\mu_B)} \right)^2 + \lambda \left(\frac{\mu_B}{T_c(\mu_B)} \right)^4 \dots$$

Recent results:

$$\kappa = 0.020(4)$$

P. Cea et al., 1508.07599

QCD phase diagram



Curvature κ defined as:

$$\frac{T_c(\mu_B)}{T_c(\mu=0)} = 1 - \kappa \left(\frac{\mu_B}{T_c(\mu_B)} \right)^2 + \lambda \left(\frac{\mu_B}{T_c(\mu_B)} \right)^4 \dots$$

Recent results:

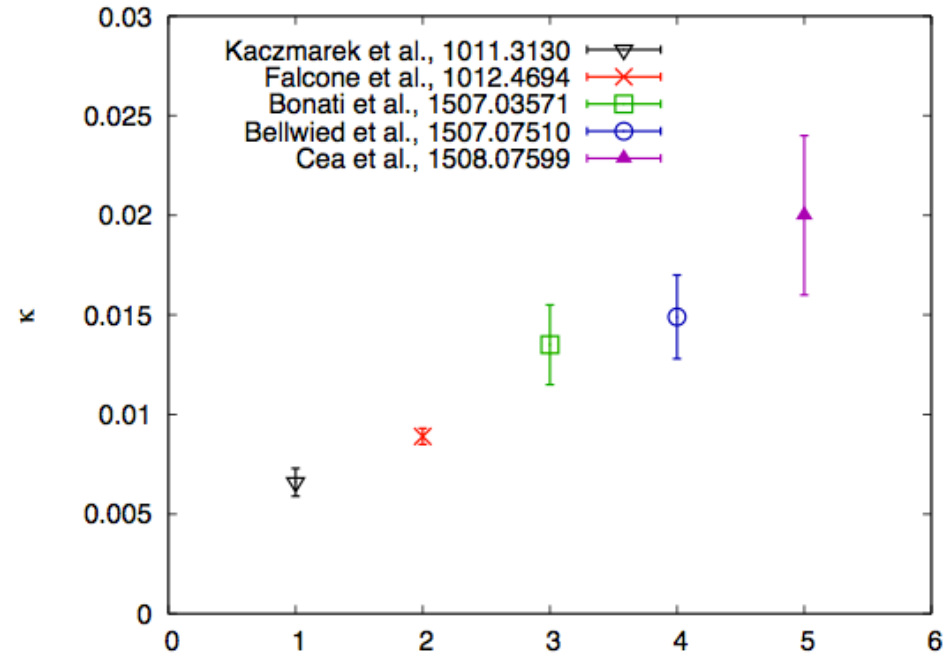
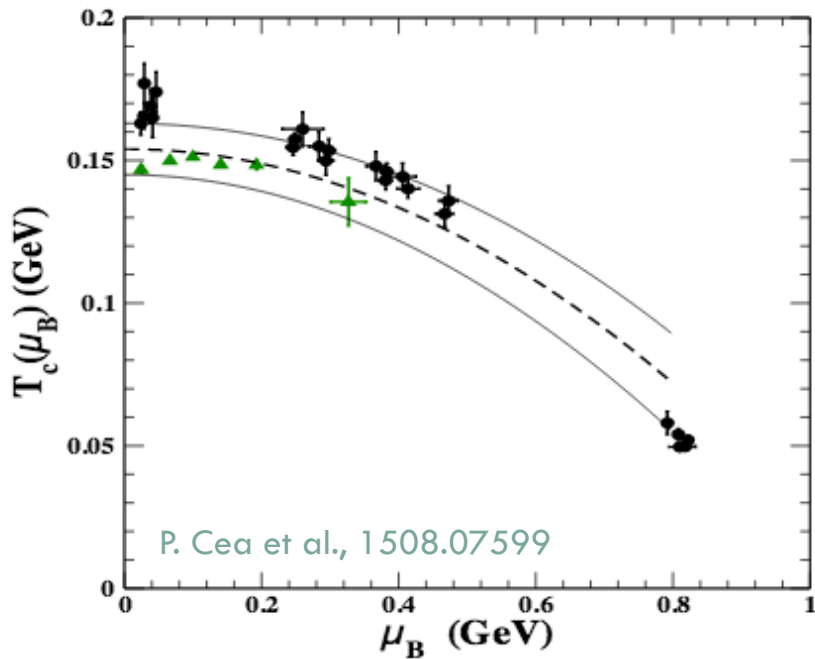
$$\kappa = 0.020(4)$$

P. Cea et al., 1508.07599

$$\kappa = 0.0135(20)$$

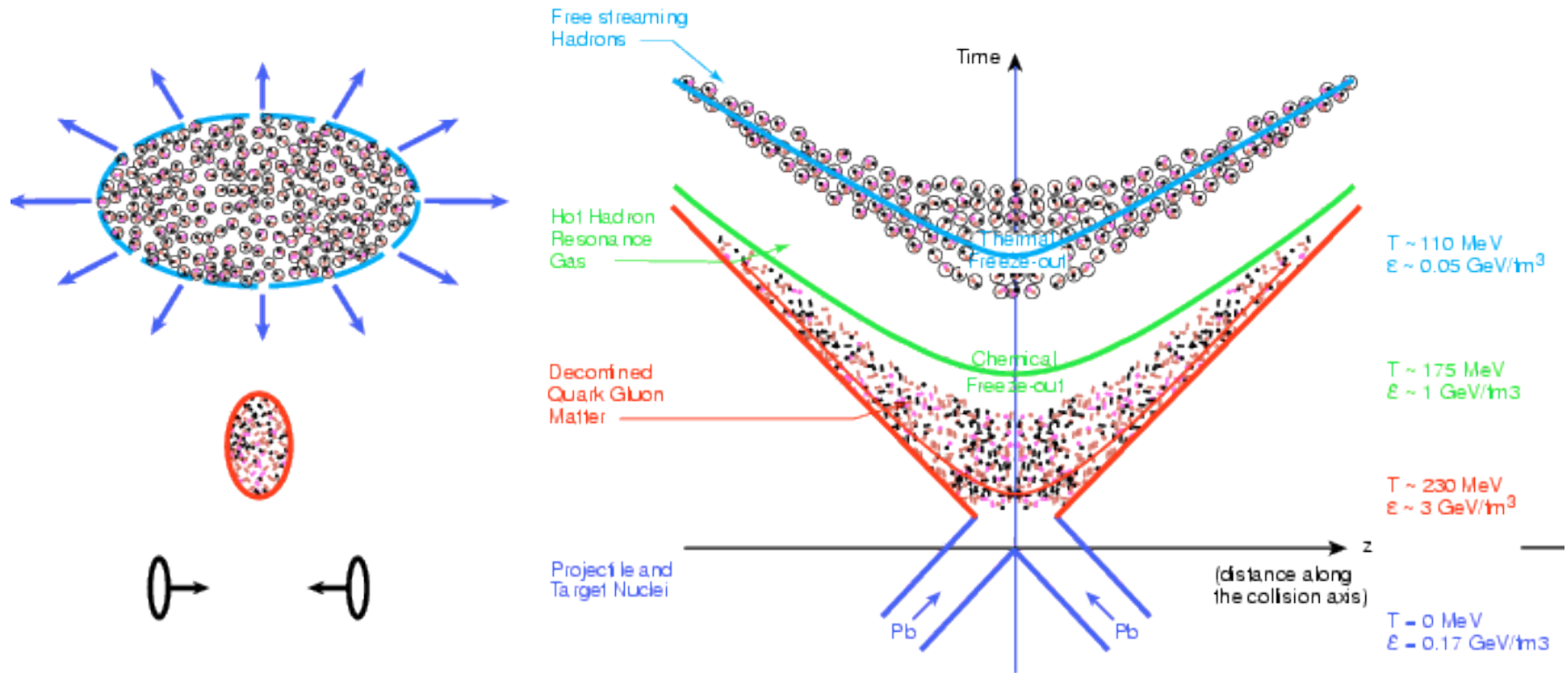
C. Bonati et al., 1507.03571

QCD phase diagram



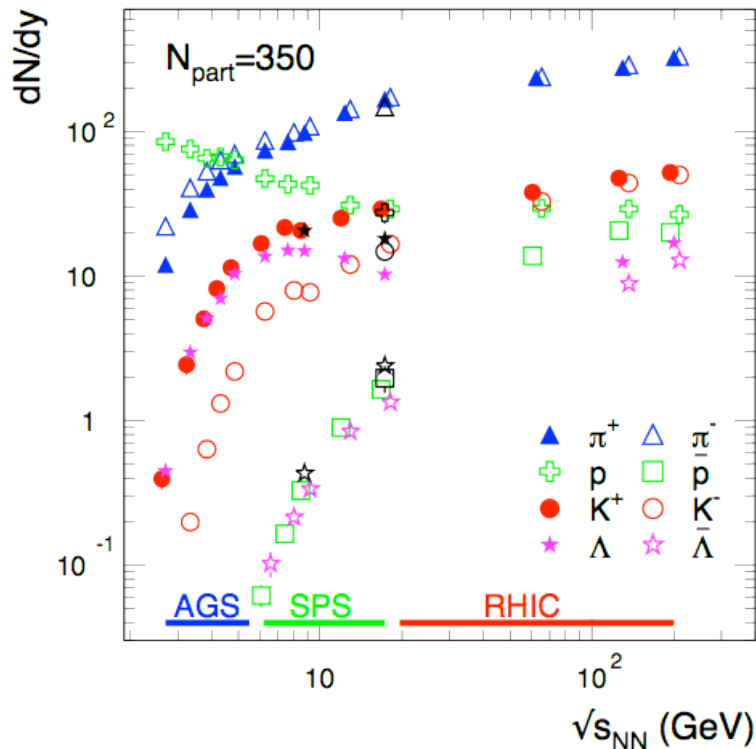
- 1 Kaczmarek et al., $N_f=2+1$, p4 staggered action, Taylor expansion, $\mu_s=0$, $N_t=8$
- 2 Falcone et al., $N_f=2+1$, p4 staggered action, analytic continuation, $\mu_s=\mu_u=\mu_d$, $N_t=4$
- 3 Bonati et al., $N_f=2+1$, stout staggered action, analytic continuation, $\mu_s=0$, continuum extrapolated
- 4 Bellwied et al. (WB), $N_f=2+1$, 4stout staggered action, analytic continuation, $\langle n_s \rangle=0$, cont. extrap.
- 5 Cea et al., $N_f=2+1$, HISQ staggered action, analytic continuation, $\mu_s=\mu_u=\mu_d$, cont. extrapolated

Evolution of a Heavy Ion Collision



- **Chemical freeze-out:** inelastic reactions cease: the chemical composition of the system is fixed (particle yields and fluctuations)
- **Kinetic freeze-out:** elastic reactions cease: spectra and correlations are frozen (free streaming of hadrons)
- Hadrons reach the detector

Hadron yields

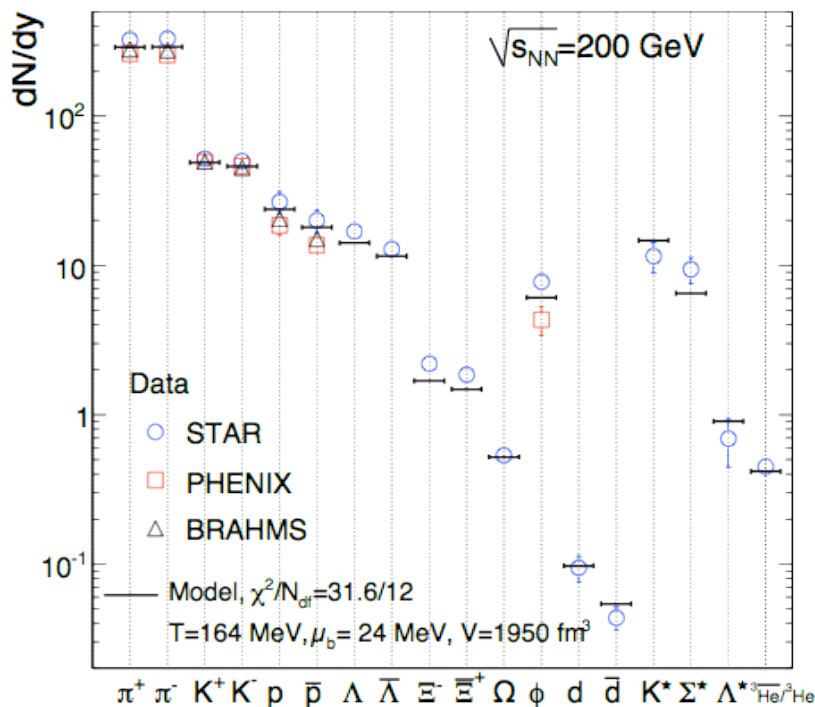


- $E=mc^2$: lots of particles are created
- **Particle counting** (average over many events)
- Take into account:
 - detector inefficiency
 - missing particles at low p_T
 - decays

- **HRG model**: test hypothesis of hadron abundancies in equilibrium

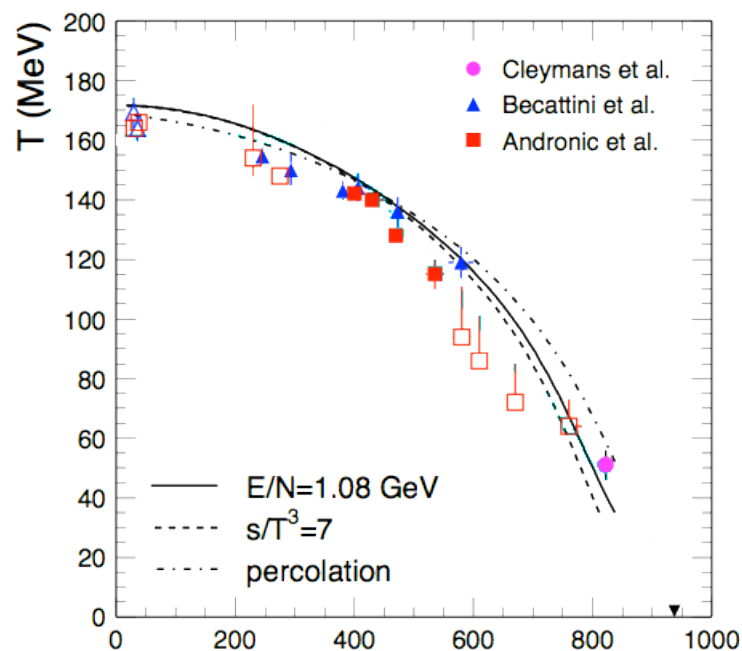
$$N_i = -T \frac{\partial \ln Z_i}{\partial \mu} = \frac{g_i V}{2\pi^2} \int_0^\infty \frac{p^2 dp}{\exp[(E_i - \mu_i)/T] \pm 1}$$

The thermal fits



- Fit is performed minimizing the χ^2
- **Fit to yields:** parameters T, μ_B, V
- **Fit to ratios:** the volume V cancels out

- Changing the collision energy, it is possible to draw the freeze-out line in the T, μ_B plane



Fluctuations of conserved charges

- Definition:

$$\chi_{lmn}^{BSQ} = \frac{\partial^{l+m+n} p / T^4}{\partial(\mu_B/T)^l \partial(\mu_S/T)^m \partial(\mu_Q/T)^n}.$$

- Relationship between chemical potentials:

$$\mu_u = \frac{1}{3}\mu_B + \frac{2}{3}\mu_Q;$$

$$\mu_d = \frac{1}{3}\mu_B - \frac{1}{3}\mu_Q;$$

$$\mu_s = \frac{1}{3}\mu_B - \frac{1}{3}\mu_Q - \mu_S.$$

- They can be calculated on the lattice and compared to experiment

Connection to experiment

- **Fluctuations** of conserved charges are the **cumulants** of their event-by-event distribution

$$\text{mean : } M = \chi_1$$

$$\text{variance : } \sigma^2 = \chi_2$$

$$\text{skewness : } S = \chi_3/\chi_2^{3/2}$$

$$\text{kurtosis : } \kappa = \chi_4/\chi_2^2$$

$$S\sigma = \chi_3/\chi_2$$

$$\kappa\sigma^2 = \chi_4/\chi_2$$

$$M/\sigma^2 = \chi_1/\chi_2$$

$$S\sigma^3/M = \chi_3/\chi_1$$

- Lattice QCD results are functions of **temperature** and **chemical potential**
 - By comparing lattice results and experimental measurement we can **extract the freeze-out parameters** from first principles

Things to keep in mind

- Effects due to volume variation because of finite centrality bin width
 - ▣ Experimentally corrected by centrality-bin-width correction method
V. Skokov et al., PRC (2013)
- Finite reconstruction efficiency
 - ▣ Experimentally corrected based on binomial distribution A.Bzdak,V.Koch, PRC (2012)
- Spallation protons
 - ▣ Experimentally removed with proper cuts in p_T
- Canonical vs Grand Canonical ensemble
 - ▣ Experimental cuts in the kinematics and acceptance V. Koch, S. Jeon, PRL (2000)
- Proton multiplicity distributions vs baryon number fluctuations
 - ▣ Recipes for treating proton fluctuations
M. Asakawa and M. Kitazawa, PRC(2012), M. Nahrgang et al., 1402.1238
- Final-state interactions in the hadronic phase
 - ▣ Consistency between different charges = fundamental test
J.Steinheimer et al., PRL (2013)

“Baryometer and Thermometer”

Let us look at the Taylor expansion of R_{31}^B

$$R_{31}^B(T, \mu_B) = \frac{\chi_3^B(T, \mu_B)}{\chi_1^B(T, \mu_B)} = \frac{\chi_4^B(T, 0) + \chi_{31}^{BQ}(T, 0)q_1(T) + \chi_{31}^{BS}(T, 0)s_1(T)}{\chi_2^B(T, 0) + \chi_{11}^{BQ}(T, 0)q_1(T) + \chi_{11}^{BS}(T, 0)s_1(T)} + \mathcal{O}(\mu_B^2)$$

- To order μ_B^2 it is independent of μ_B : it can be used as a **thermometer**
- Let us look at the Taylor expansion of R_{12}^B

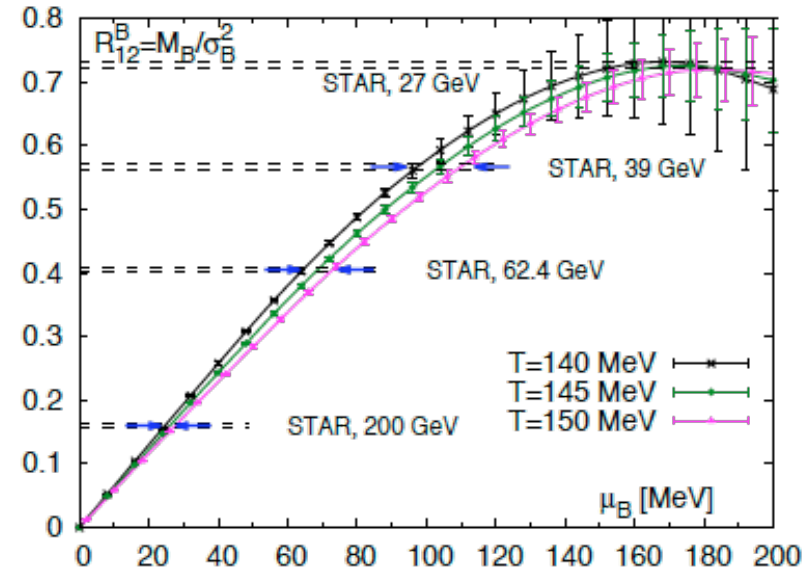
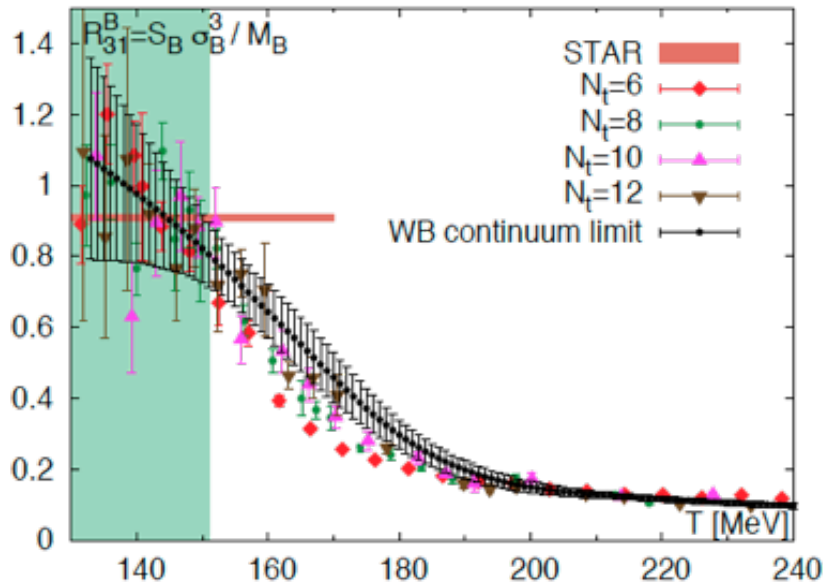
$$R_{12}^B(T, \mu_B) = \frac{\chi_1^B(T, \mu_B)}{\chi_2^B(T, \mu_B)} = \frac{\chi_2^B(T, 0) + \chi_{11}^{BQ}(T, 0)q_1(T) + \chi_{11}^{BS}(T, 0)s_1(T)}{\chi_2^B(T, 0)} \frac{\mu_B}{T} + \mathcal{O}(\mu_B^3)$$

- Once we extract T from R_{31}^B , we can use R_{12}^B to extract μ_B

Freeze-out parameters from B fluctuations

Thermometer: $\frac{\chi_3^B(T, \mu_B)}{\chi_1^B(T, \mu_B)} = S_B \sigma_B^3 / M_B$

Baryometer: $\frac{\chi_1^B(T, \mu_B)}{\chi_2^B(T, \mu_B)} = \sigma_B^2 / M_B$



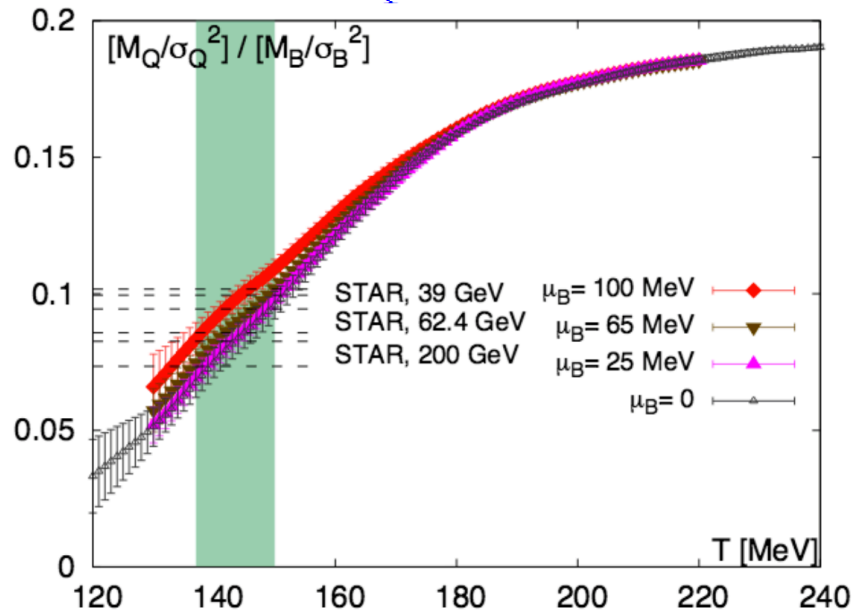
WB: S. Borsanyi et al., PRL (2014)
STAR collaboration, PRL (2014)

Upper limit: $T_f \leq 151 \pm 4$ MeV

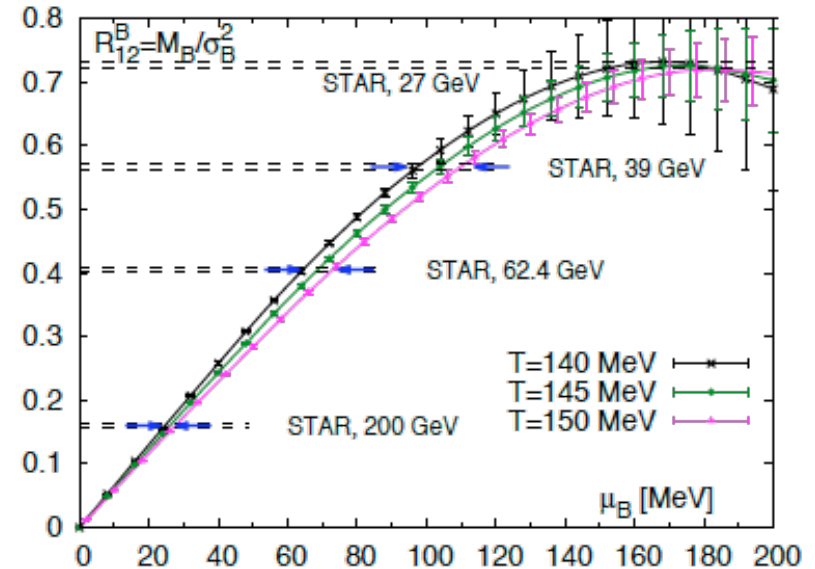
Consistency between freeze-out chemical potential from electric charge and baryon number is found.

Freeze-out parameters from B fluctuations

Thermometer: $\frac{\chi_3^B(T, \mu_B)}{\chi_1^B(T, \mu_B)} = S_B \sigma_B^3 / M_B$



Baryometer: $\frac{\chi_1^B(T, \mu_B)}{\chi_2^B(T, \mu_B)} = \sigma_B^2 / M_B$



Upper limit: $T_f \leq 151 \pm 4$ MeV

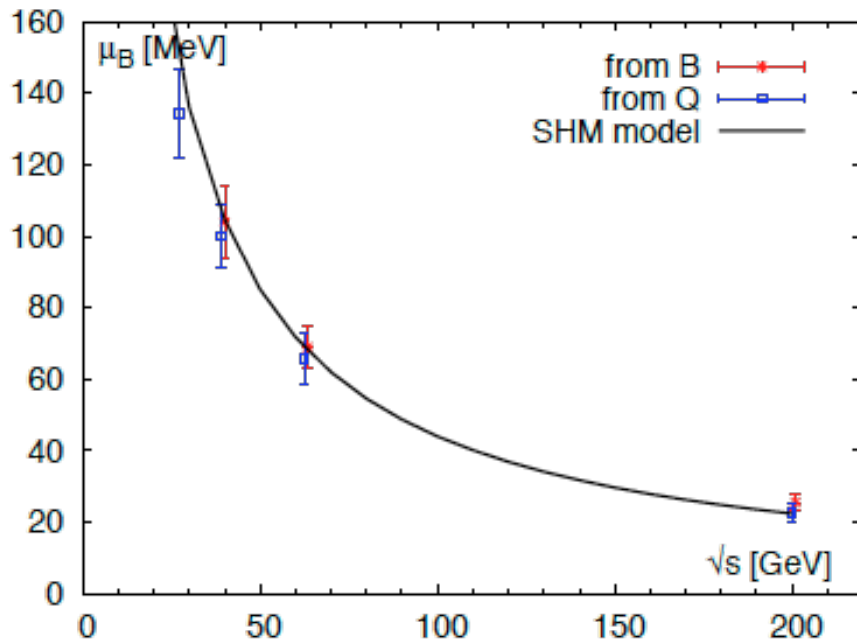
Consistency between freeze-out chemical potential from electric charge and baryon number is found.

WB: S. Borsanyi et al., PRL (2014)
STAR collaboration, PRL (2014)

Freeze-out parameters from B fluctuations

Thermometer: $\frac{\chi_3^B(T, \mu_B)}{\chi_1^B(T, \mu_B)} = S_B \sigma_B^3 / M_B$

Baryometer: $\frac{\chi_1^B(T, \mu_B)}{\chi_2^B(T, \mu_B)} = \sigma_B^2 / M_B$



$\sqrt{s} [GeV]$	$\mu_B^f [MeV]$ (from B)	$\mu_B^f [MeV]$ (from Q)
200	25.8 ± 2.7	22.8 ± 2.6
62.4	69.7 ± 6.4	66.6 ± 7.9
39	105 ± 11	101 ± 10
27	-	136 ± 13.8

WB: S. Borsanyi et al., PRL (2014)
STAR collaboration, PRL (2014)

Upper limit: $T_f \leq 151 \pm 4$ MeV

Consistency between freeze-out chemical potential from electric charge and baryon number is found.

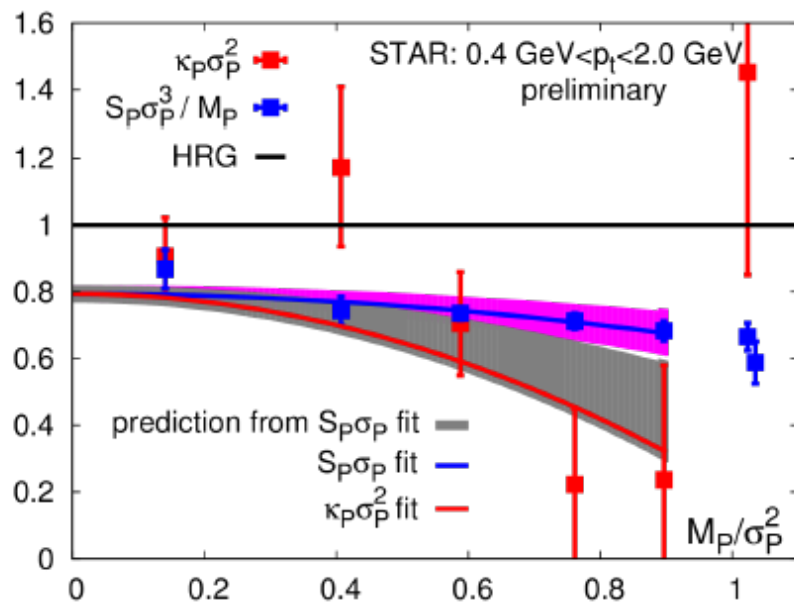
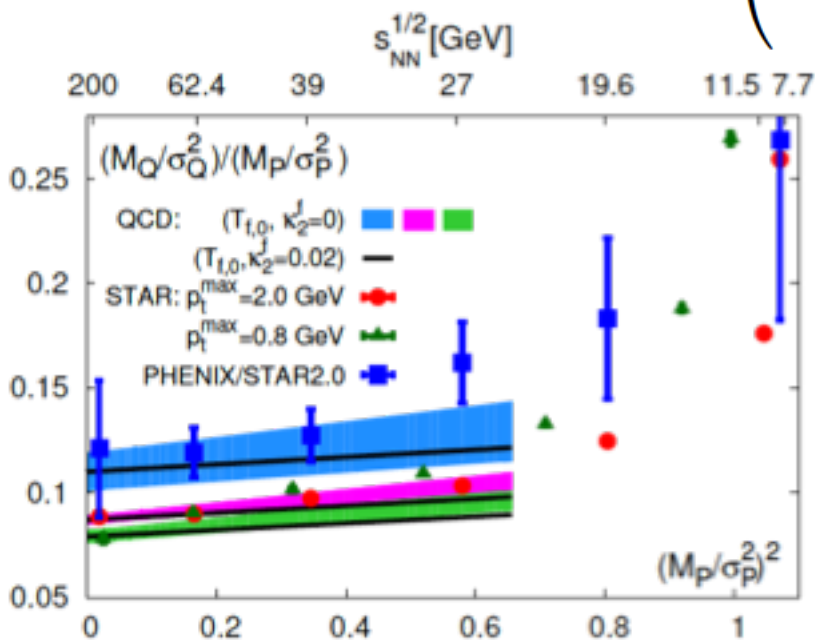
Curvature of the freeze-out line

- Parametrization of the freeze-out line:

$$T_f(\mu_B) = T_{f,0} \left(1 - \kappa_2^f \bar{\mu}_B^2 - \kappa_4^f \bar{\mu}_B^4 \right)$$

- Taylor expansion of the “ratio of ratios” $R_{12}^{QB} = [M_Q/\sigma_Q^2]/[M_B/\sigma_B^2]$

$$R_{12}^{QB} = R_{12}^{QB,0} + \left(R_{12}^{QB,2} - \kappa_2^f T_{f,0} \frac{dR_{12}^{QB,0}}{dT} \Big|_{T_{f,0}} \right) \hat{\mu}_B^2$$



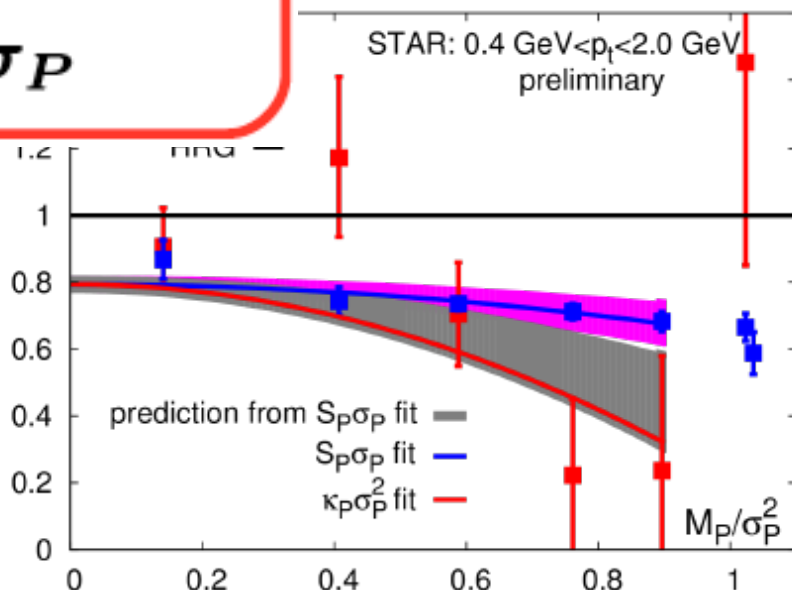
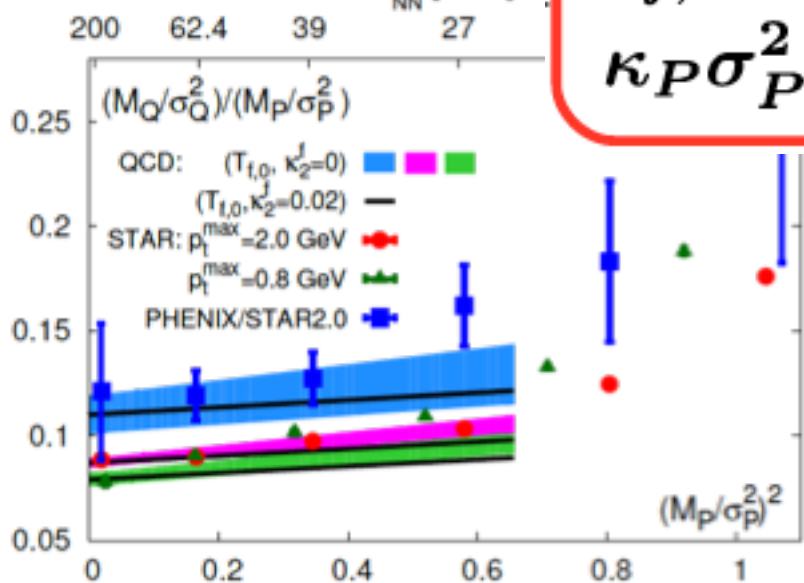
Curvature of the freeze-out line

- Parametrization of the freeze-out line:

$$T_f(\mu_B) = T_{f,0} \left(1 - \kappa_2^f \bar{\mu}_B^2 - \kappa_4^f \bar{\mu}_B^4 \right)$$

- Taylor expansion of the “ratio of ratios” $R_{12}^{QB} = [M_Q/\sigma_Q^2]/[M_B/\sigma_B^2]$

$$R_{12}^{QB} = \left(\begin{array}{l} \kappa_2^f < 0.011 \\ T_{f,0} = (147 \pm 2) \text{ MeV} \\ \kappa_P \sigma_P^2 < S_P \sigma_P \end{array} \right) \hat{\mu}_B^2$$



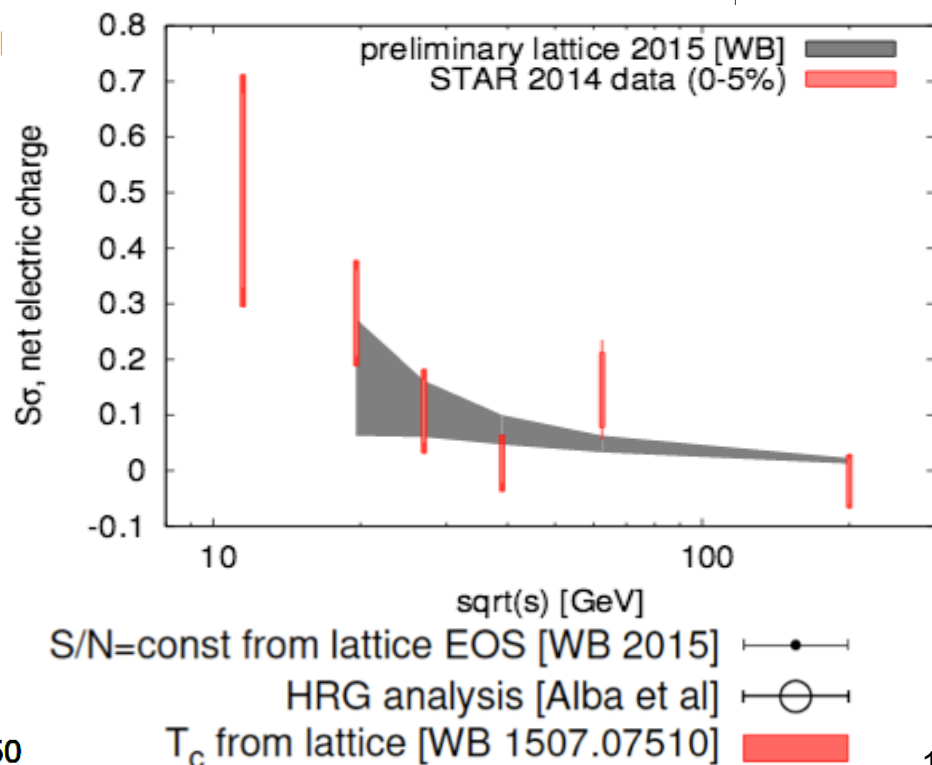
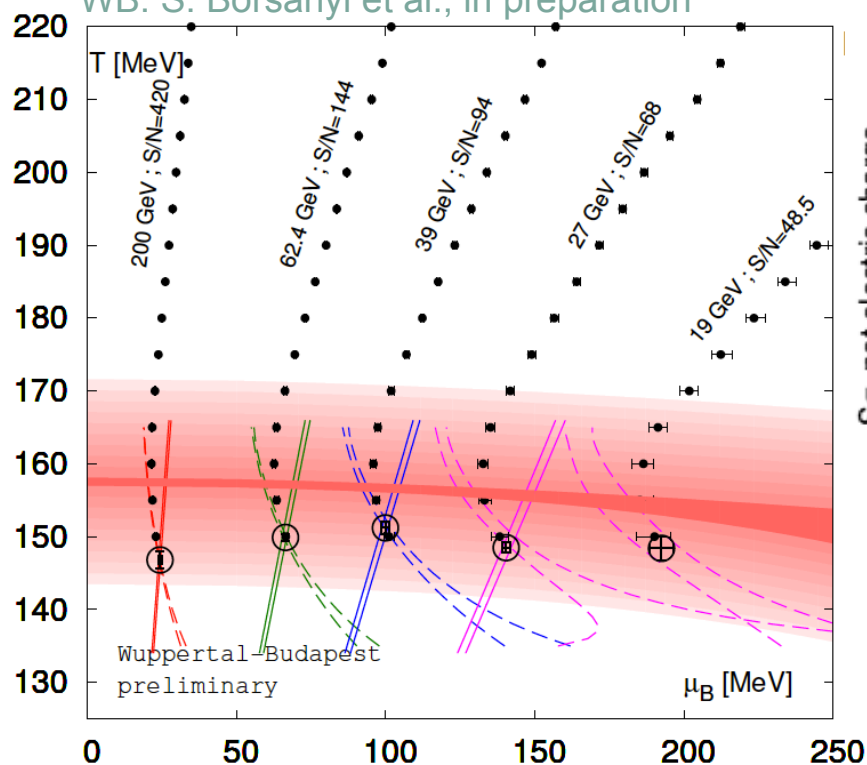
Freeze-out line from first principles

- Use T - and μ_B -dependence of R_{12}^Q and R_{12}^B for a combined fit:

$$R_{12}^Q(T, \mu_B) = \frac{\chi_1^Q(T, \mu_B)}{\chi_2^Q(T, \mu_B)} = \frac{\chi_{11}^{QB}(T, 0) + \chi_2^Q(T, 0)q_1(T) + \chi_{11}^{QS}(T, 0)s_1(T)}{\chi_2^Q(T, 0)} \frac{\mu_B}{T} + \mathcal{O}(\mu_B^3).$$

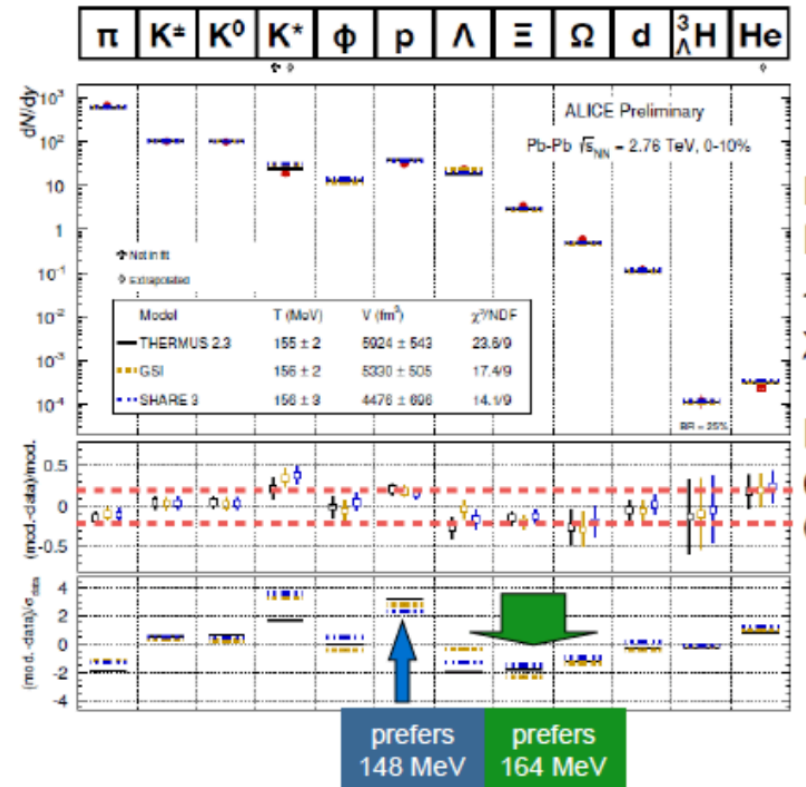
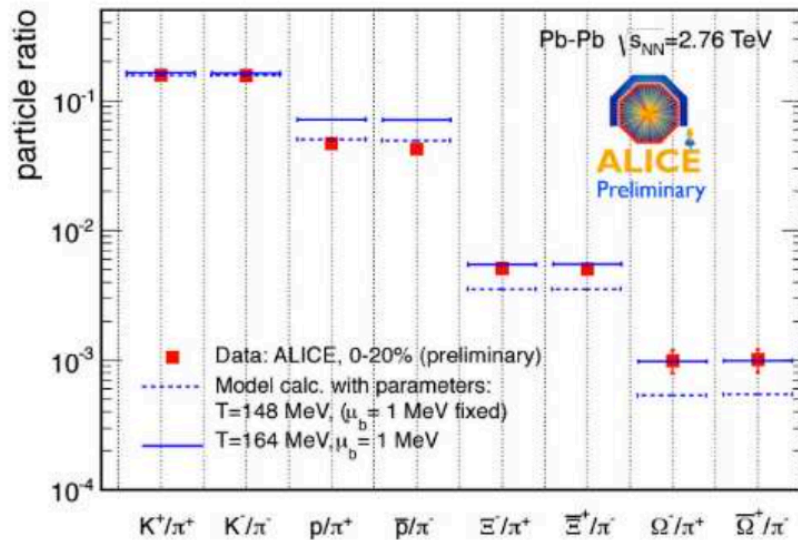
$$R_{12}^B(T, \mu_B) = \frac{\chi_1^B(T, \mu_B)}{\chi_2^B(T, \mu_B)} = \frac{\chi_2^B(T, 0) + \chi_{11}^{BQ}(T, 0)q_1(T) + \chi_{11}^{BS}(T, 0)s_1(T)}{\chi_2^B(T, 0)} \frac{\mu_B}{T} + \mathcal{O}(\mu_B^3)$$

WB: S. Borsanyi et al., in preparation



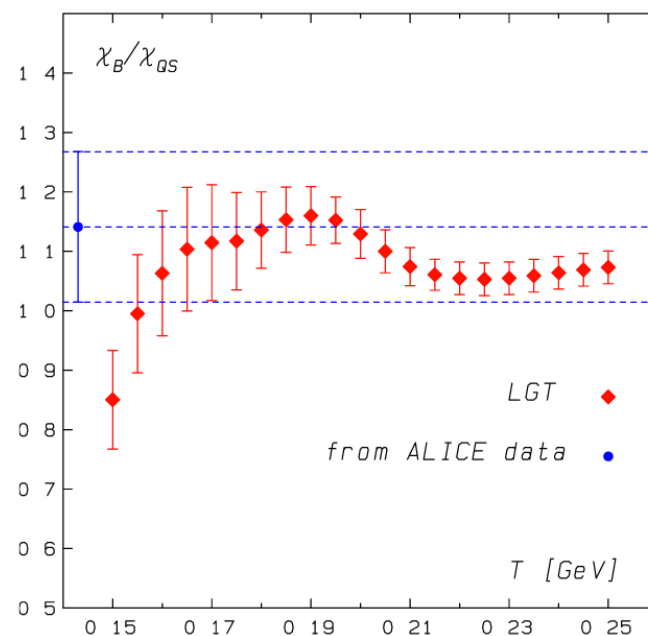
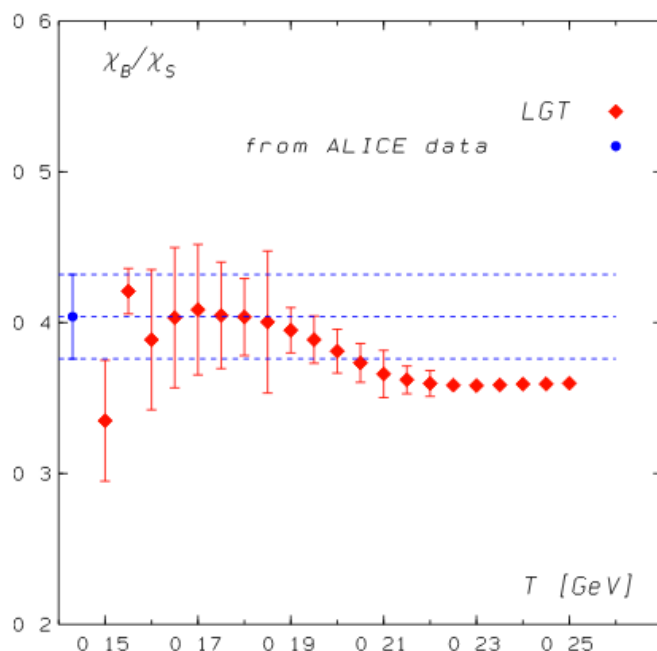
What about strangeness freeze-out?

- Yield fits seem to hint at a higher temperature for strange particles



Initial analysis of LHC data

- Fluctuation data not yet available
- Assuming Skellam distribution, can use yields: $\hat{\chi}_N = \frac{1}{\sqrt{T^3}} \left(\langle N_q \rangle + \langle N_{-q} \rangle \right)$

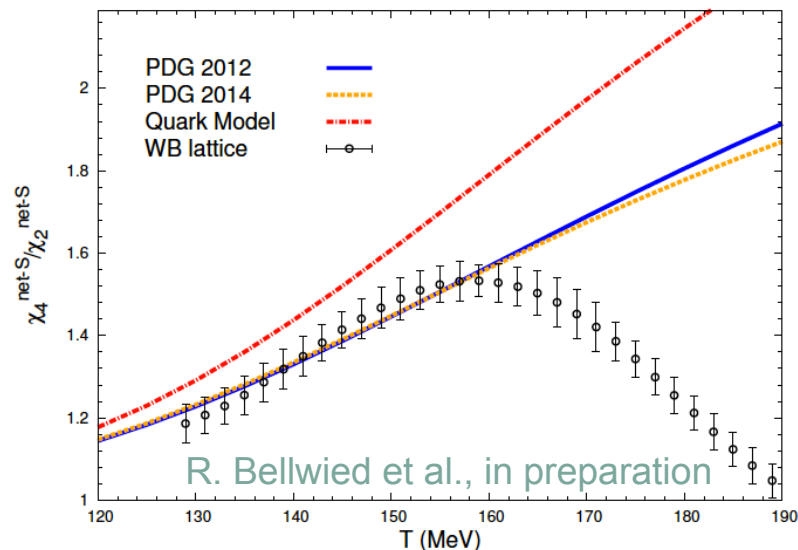
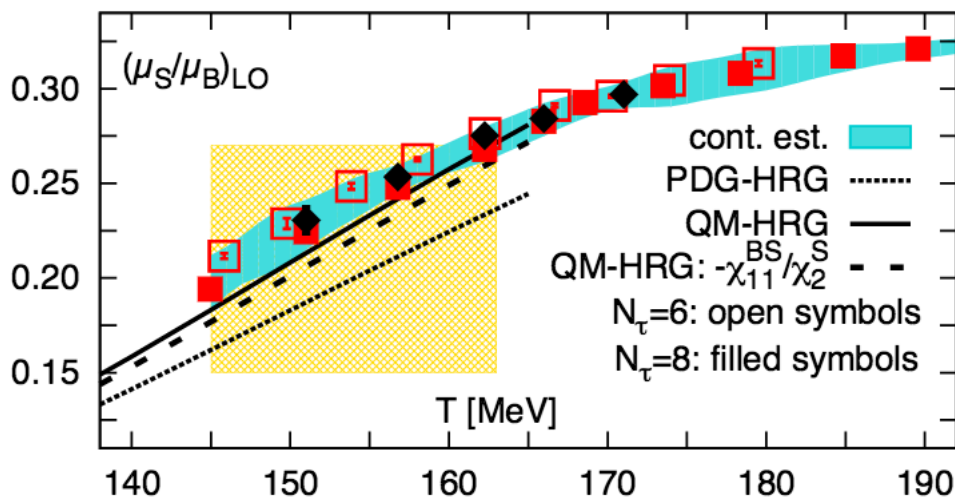


P. Braun-Munzinger et al., PLB (2015)

- Slightly higher temperature than at RHIC: ($150 < T_f < 163$) MeV
- Looking forward to fluctuation measurements at the LHC

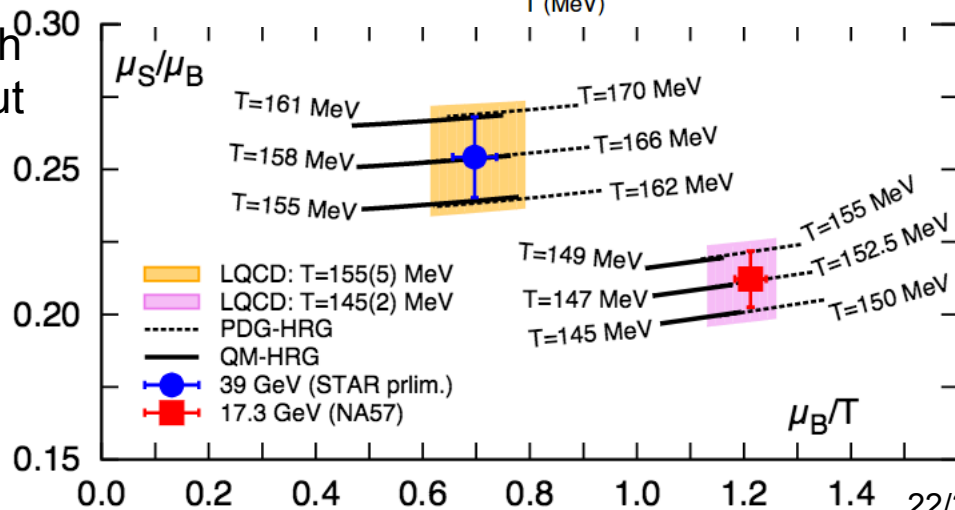
Missing strange states?

- Quark Model predicts not-yet-detected (multi-)strange hadrons



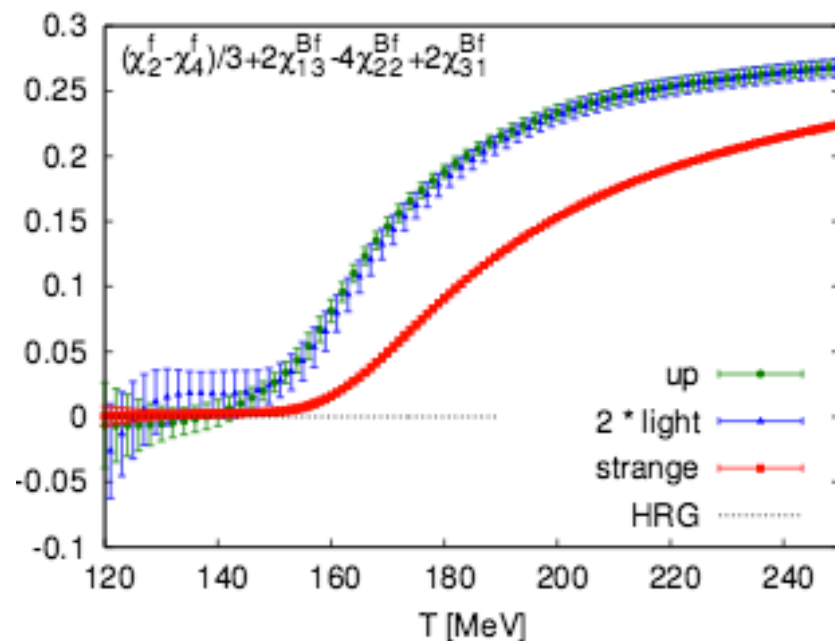
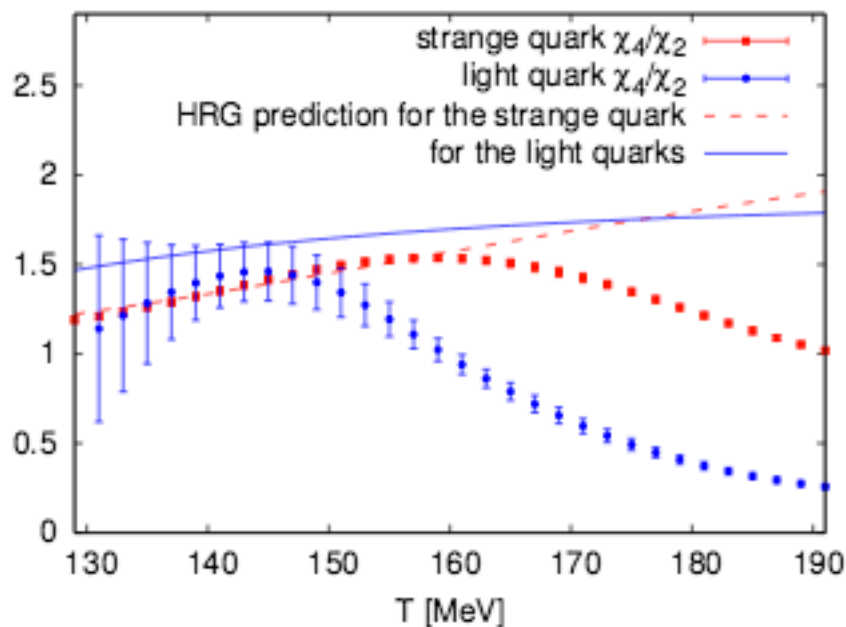
- QM-HRG improves the agreement with lattice results for some observables but it worsens it for some other ones
- The effect is only relevant at finite μ_B
- Feed-down from resonance decays neglected

A. Bazavov et al., PRL (2014)



Flavor-dependent freeze-out?

WB: R. Bellwied et al, PRL (2013)

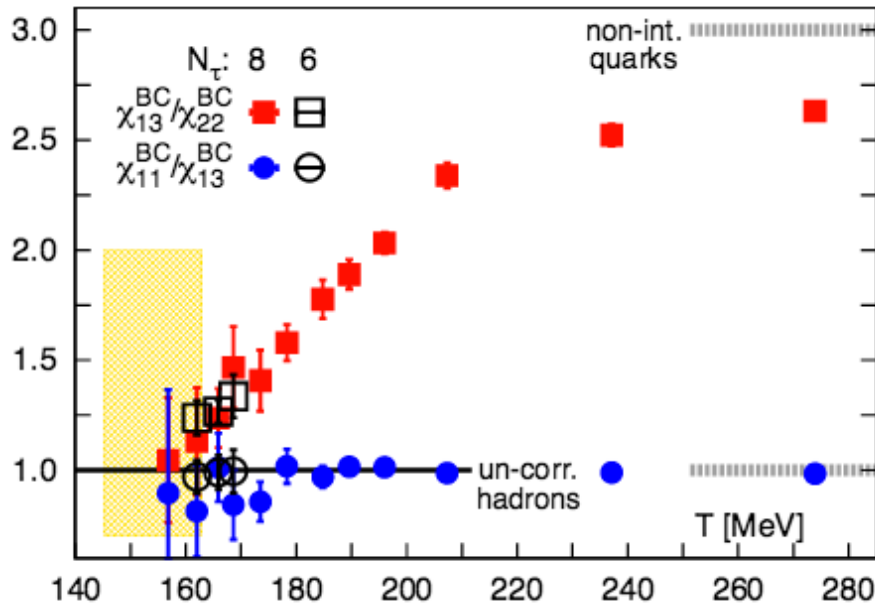


- Lattice data hint at possible flavor-dependence in transition temperature
- Possibility of strange bound-states above T_c ?

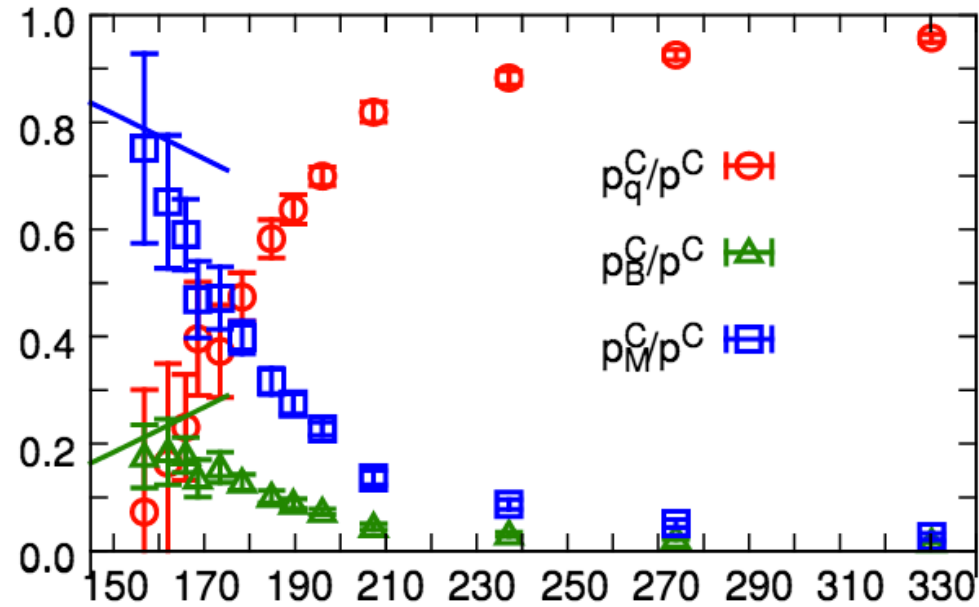
See talk by R. Bellwied on Thursday

Degrees of freedom from fluctuations

- Onset of deconfinement for charm quarks:



A. Bazavov et al., PLB (2014)

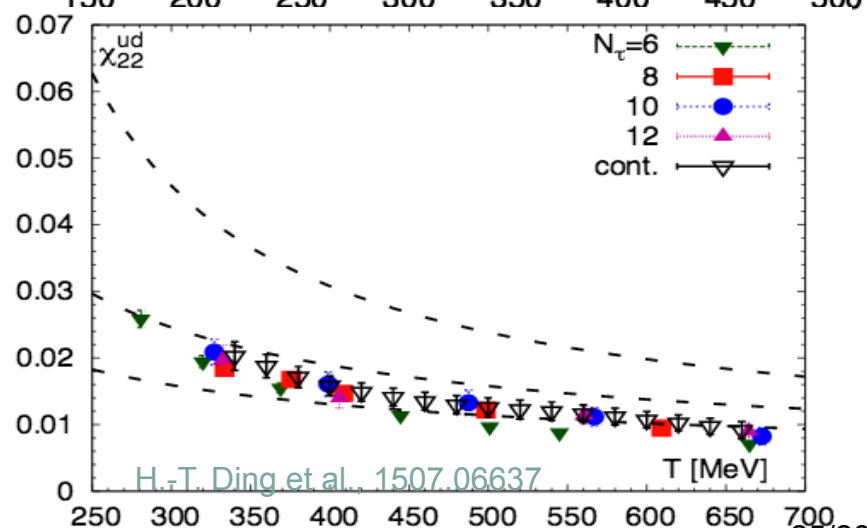
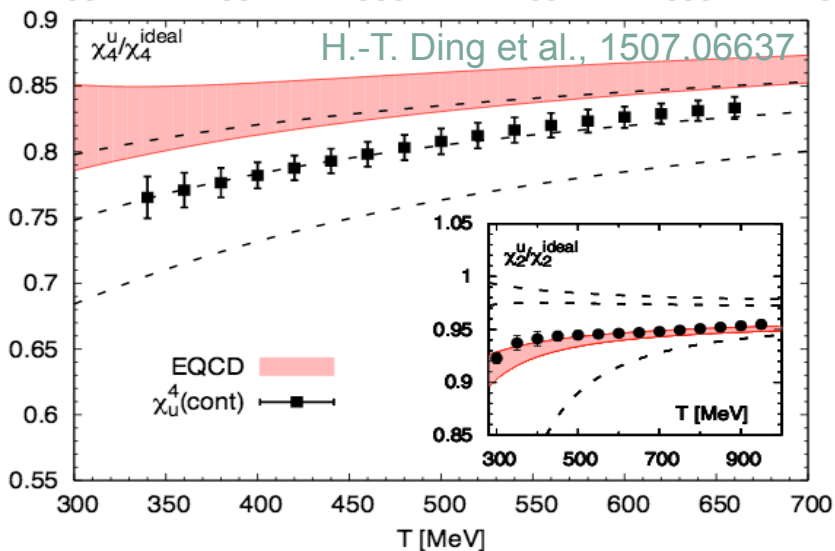
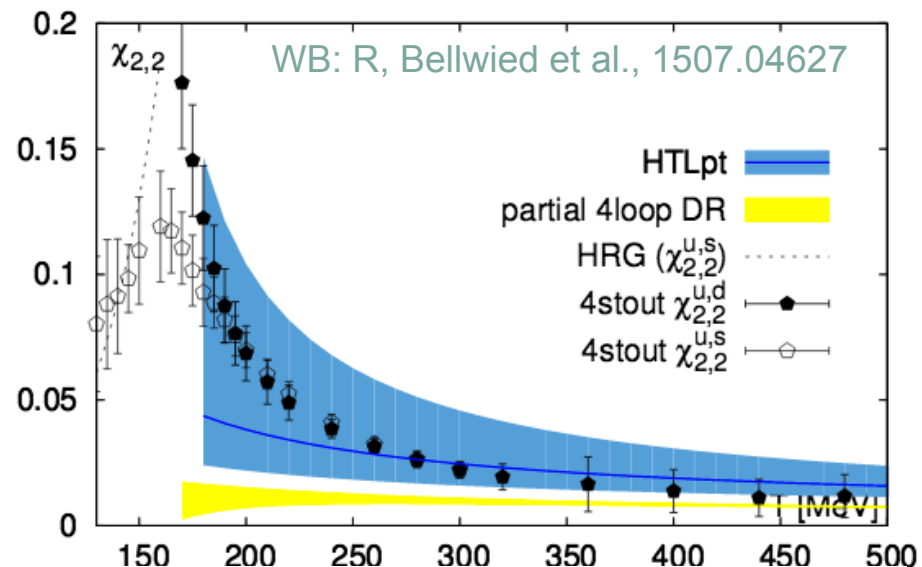
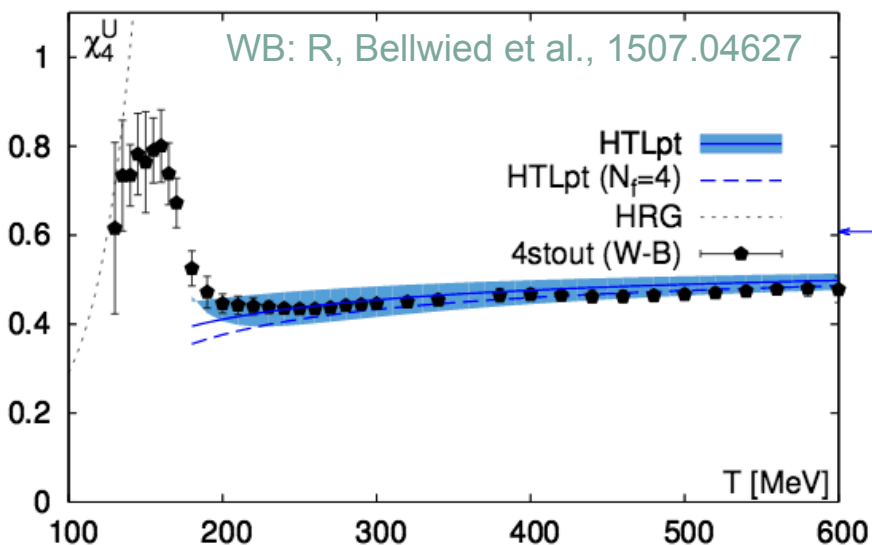


S. Mukherjee, P. Petreczky, S. Sharma 1509.08887

- Partial meson and baryon pressures described by HRG at T_C and dominate the charm pressure then drop gradually. Charm quark only dominant dof at $T > 200$ MeV

Fluctuations at high temperatures

HTL: N. Haque et al., JHEP (2014); DR: S. Mogliacci et al., JHEP (2013)



Conclusions

- Unprecedented precision in lattice QCD data allows a direct comparison to experiment for the first time
- QCD thermodynamics at $\mu_B=0$ can be simulated with high accuracy
- Extensions to finite density are under control up to $O(\mu_B^6)$
- Challenges for the near future
 - ▣ Sign problem
 - ▣ Real-time dynamics

Transport properties

- Matter in the region $(1-2)T_c$ is highly non-perturbative
- Significant modifications of its transport properties
- Common problem:
 - ▣ Transport properties can be explored through the analysis of certain correlation functions:

$$G_H(\tau, \vec{p}, T) = \int_0^\infty \frac{d\omega}{2\pi} \rho_H(\omega, \vec{p}, T) \frac{\cosh(\omega(\tau - 1/2T))}{\sinh(\omega/2T)} = \int d^3x e^{i\vec{p}\cdot\mathbf{x}} \langle J^\alpha(0, 0) J^{\beta\dagger}(\tau, \mathbf{x}) \rangle$$

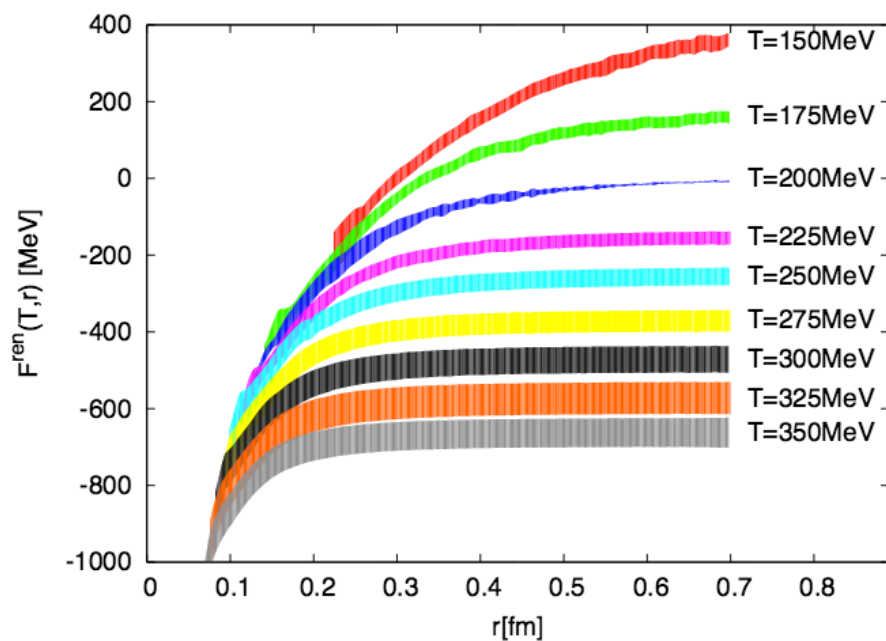
- ▣ **Challenge:** integrate over discrete set of lattice points in τ direction
- ▣ Use inversion methods like Maximum Entropy Method or modeling the spectral function at low frequencies

Quarkonia properties

- Three main approaches:
 - **Potential models** with heavy quark potential calculated on the lattice
 - Solve Schroedinger's equation for the bound state two-point function
 - Extract **spectral functions** from Euclidean temporal correlators
 - Study **spatial correlation functions** of quarkonia and their in-medium screening properties

Inter-quark potential

- Static quark-antiquark free-energy

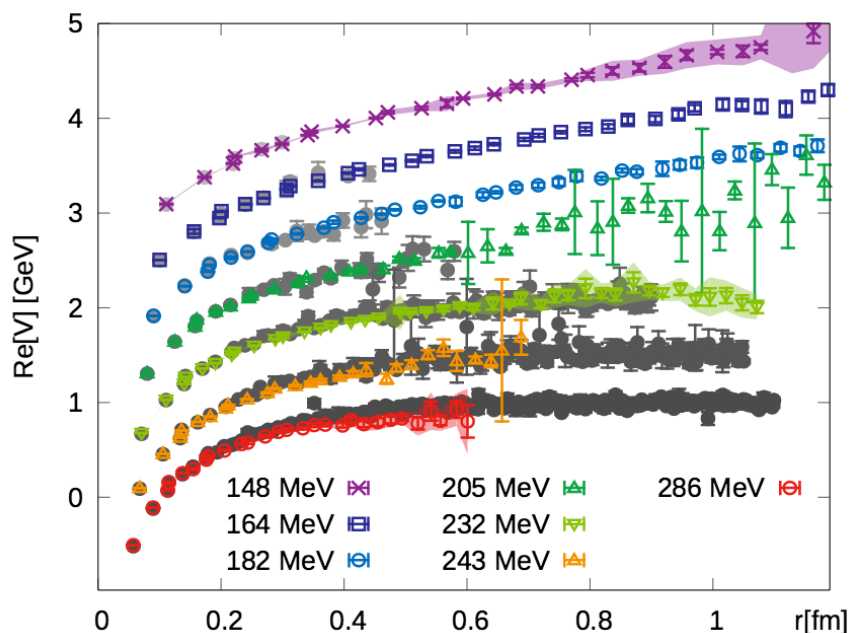


Borsanyi et al. JHEP(2015)

- Continuum extrapolated result with $N_f=2+1$ flavors at the physical mass

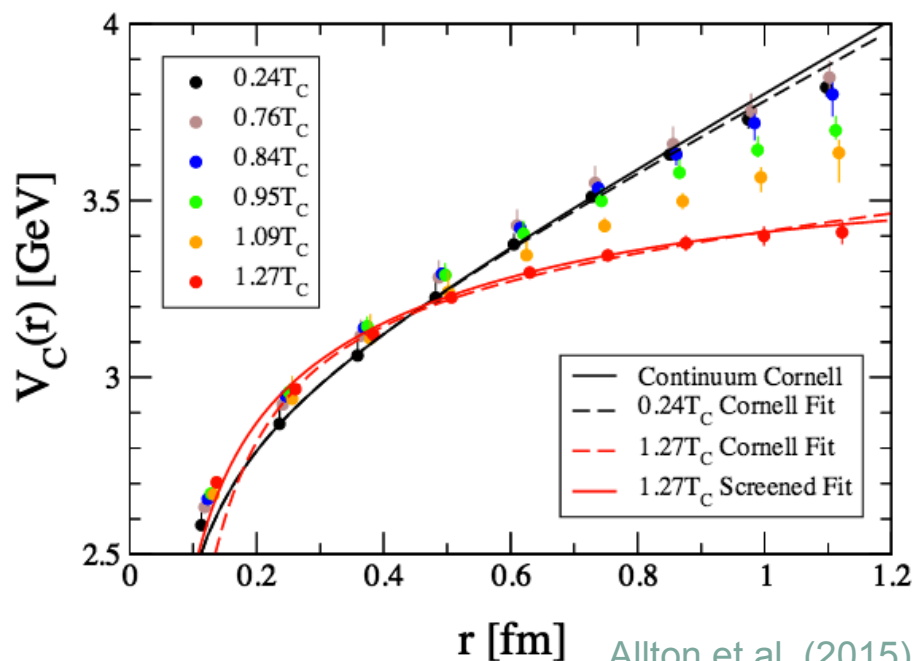
Inter-quark potential

Quark-antiquark potential in $N_f=2+1$ QCD



Burnier et al. (2014)

Real part of the complex potential lies close to the color singlet free energy



Allton et al. (2015)

Central potential: combination of pseudoscalar and vector potentials:

$$V_C(\mathbf{r}) = \frac{1}{4}V_{PS} + \frac{3}{4}V_V$$

Quarkonia spectral functions

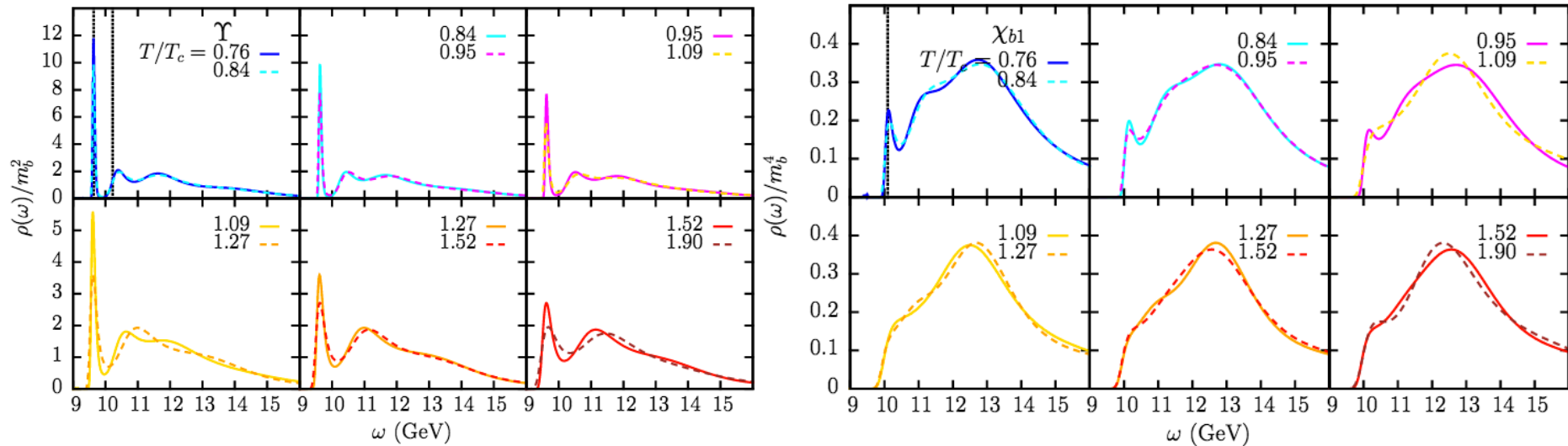
- Charmonium spectral functions in quenched approximation and preliminary studies with dynamical quarks yield consistent results: all charmonium states are dissociated for $T \gtrsim 1.5 T_c$

H. Ding et al., PRD (2012)

G. Aarts et al., PRD (2007)

WB: S. Borsanyi et al., JHEP (2014)

- Bottomonium ($N_f=2+1$, $m_\pi=400$ MeV), MEM:



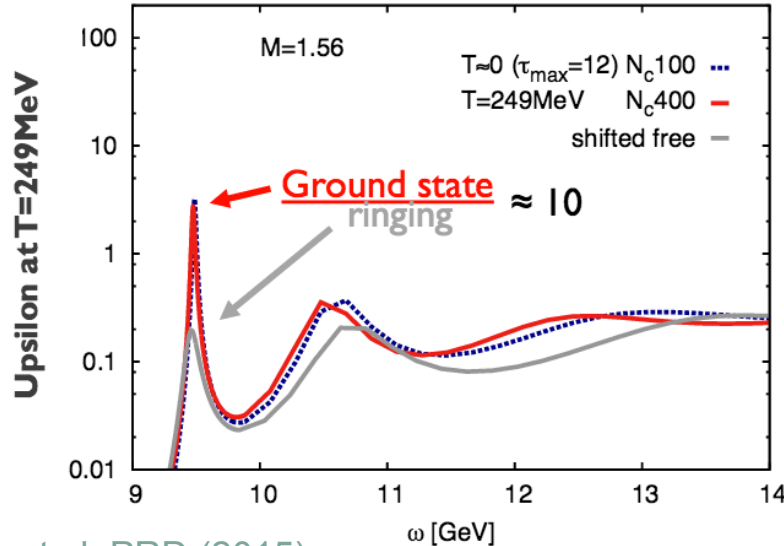
G. Aarts et al. JHEP (2014)

- S-wave ground state survives up to $1.9 T_c$, P-wave ground state melts just above T_c

Quarkonia spectral functions

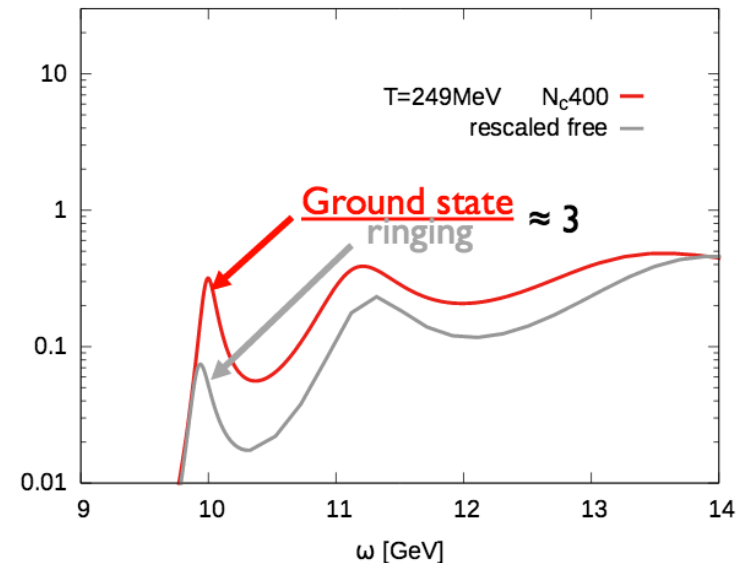
- Charmonium spectral functions in quenched approximation and preliminary studies with dynamical quarks yield consistent results: all charmonium states are dissociated for $T \gtrsim 1.5T_c$
 - H. Ding et al., PRD (2012)
 - G. Aarts et al., PRD (2007)
 - WB: S. Borsanyi et al., JHEP (2014)
- Bottomonium ($N_f=2+1$, $m_\pi=160$ MeV), Bayesian method:

$\Upsilon(1S)$ signal survives at $T=249$ MeV



S. Kim et al. PRD (2015)

$\chi_b(1P)$ signal survives at $T=249$ MeV



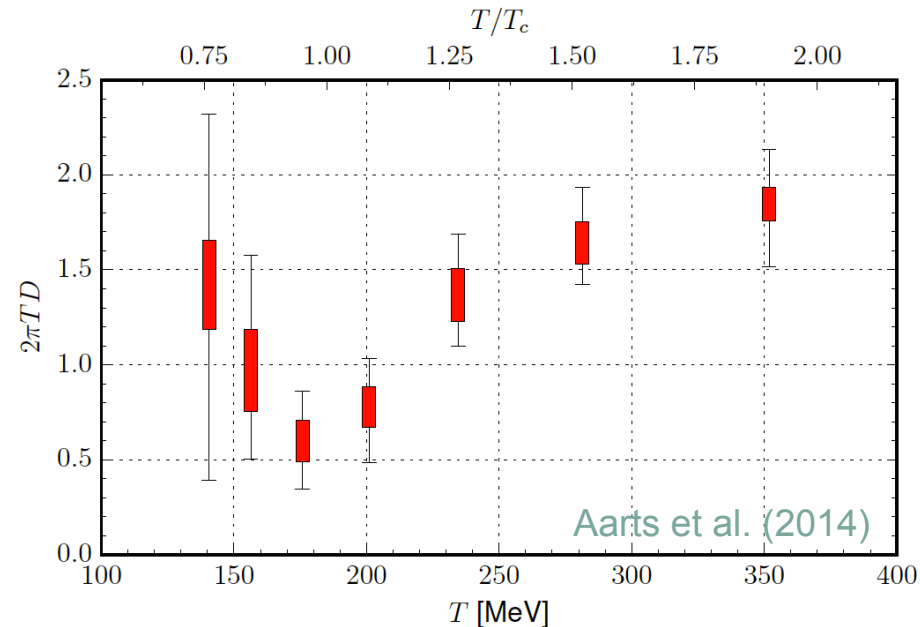
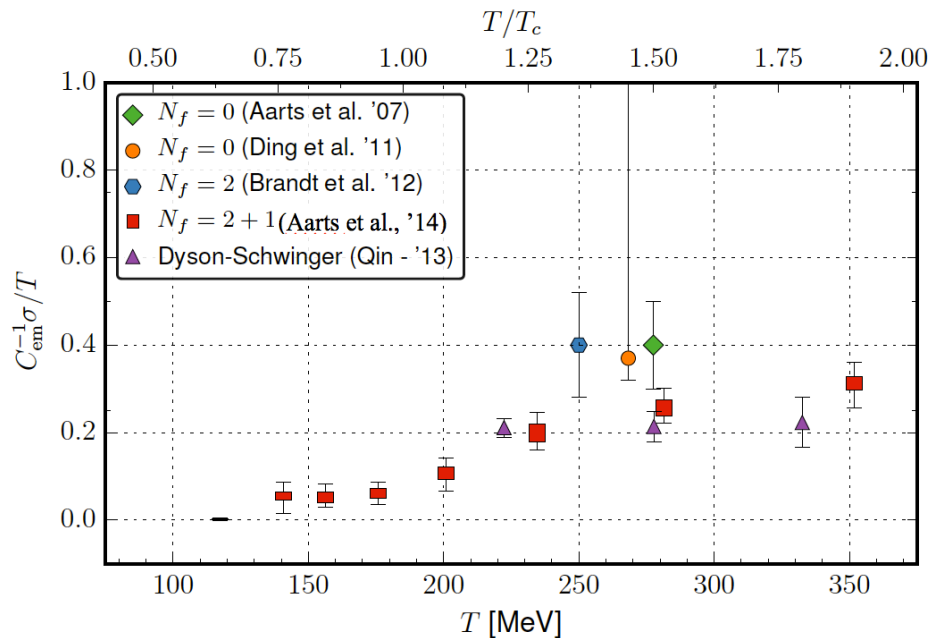
- S-wave ground state and P-wave ground state survive up to $T \sim 250$ MeV

Electric conductivity and charge diffusion

- Definitions:

$$\sigma = \frac{C_{em}}{6} \lim_{\omega \rightarrow 0} \lim_{\mathbf{p} \rightarrow 0} \sum_{i=1}^3 \frac{\rho^{ii}(\omega, \mathbf{p}, T)}{\omega}$$

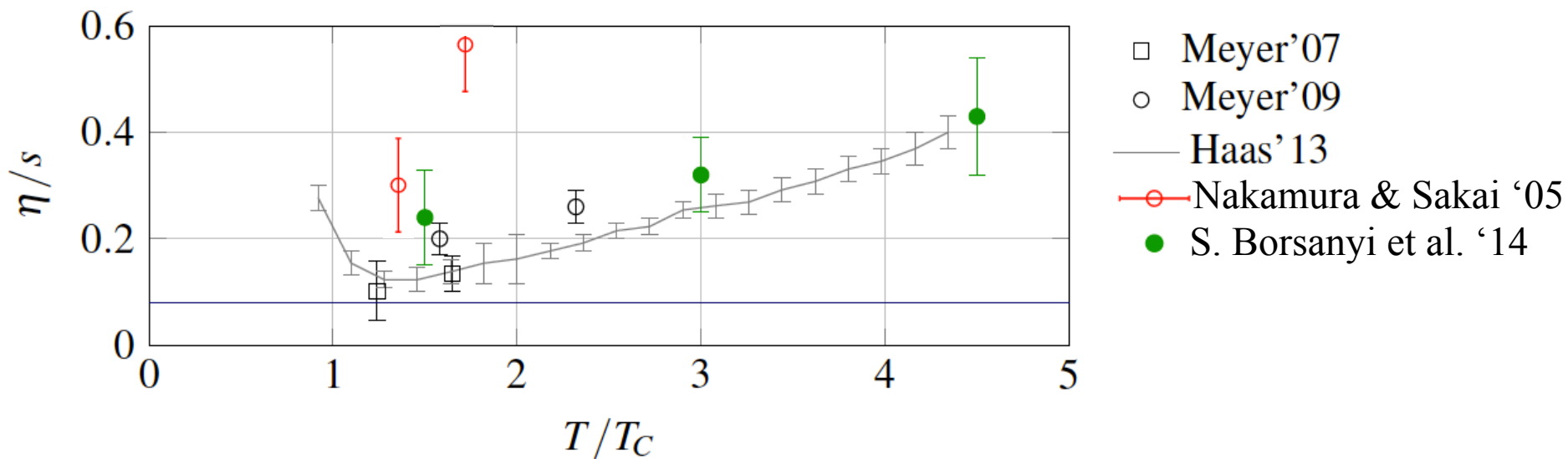
$$D_Q = \sigma / \chi_2^Q$$



- Electric conductivity measures the response of the medium to small perturbations induced by an electromagnetic field

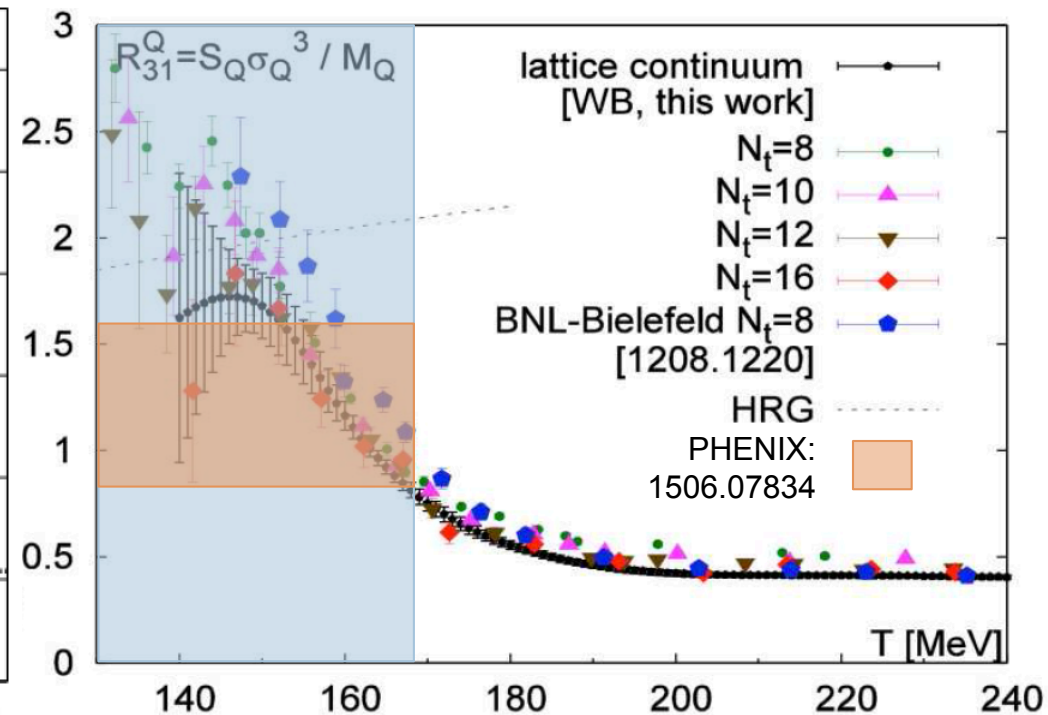
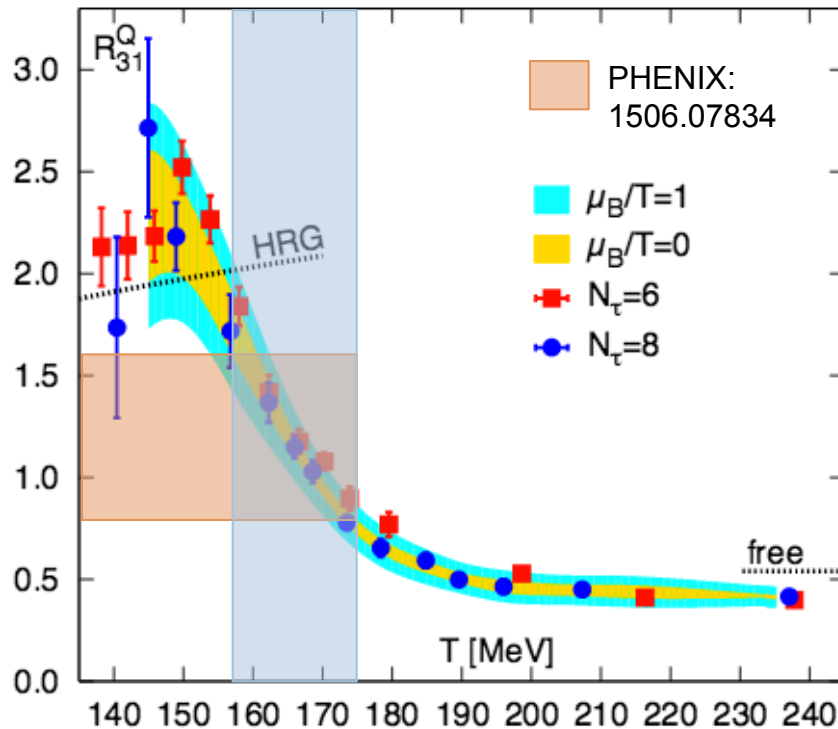
Viscosity

- Shear viscosity in the pure gauge sector of QCD



- Challenge: very low signal-to noise ratio for the Euclidean energy-momentum correlator

Freeze-out parameters from Q fluctuations



A. Bazavov et al. (2014)

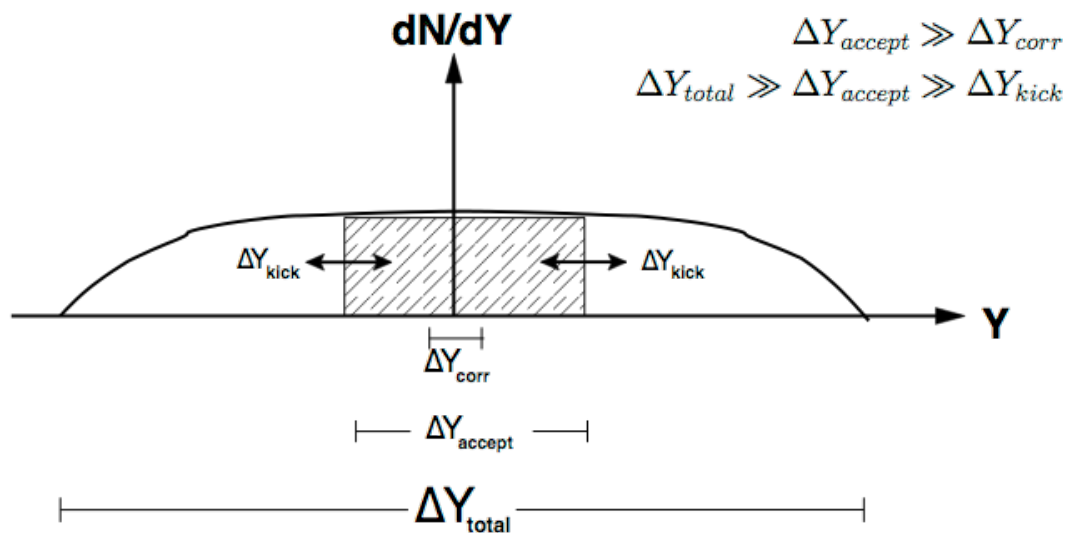
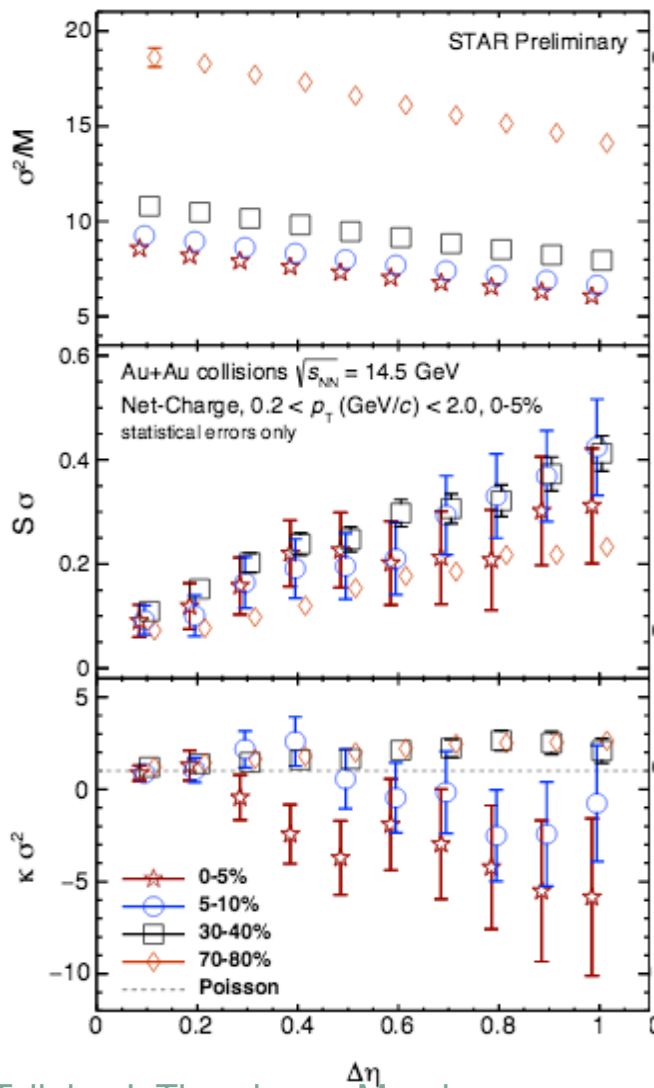
WB: Borsanyi et al. PRL (2013)

F. Karsch et al., 1508.02614

Studies in HRG model: the different momentum cuts between STAR and PHENIX are responsible for more than 30% of their difference

Using continuum extrapolated lattice data, lower values for T_f are found

Effects of kinematic cuts



V. Koch, 0810.2520

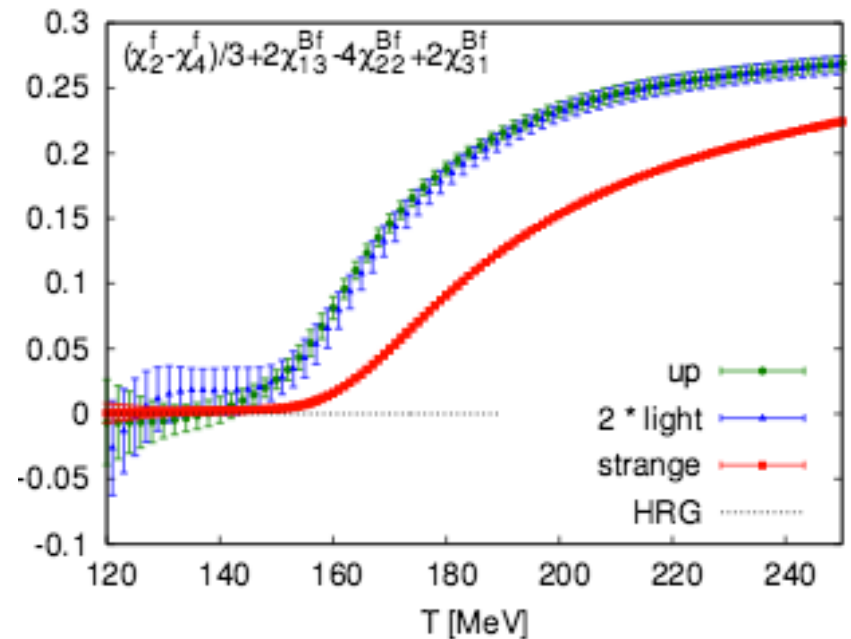
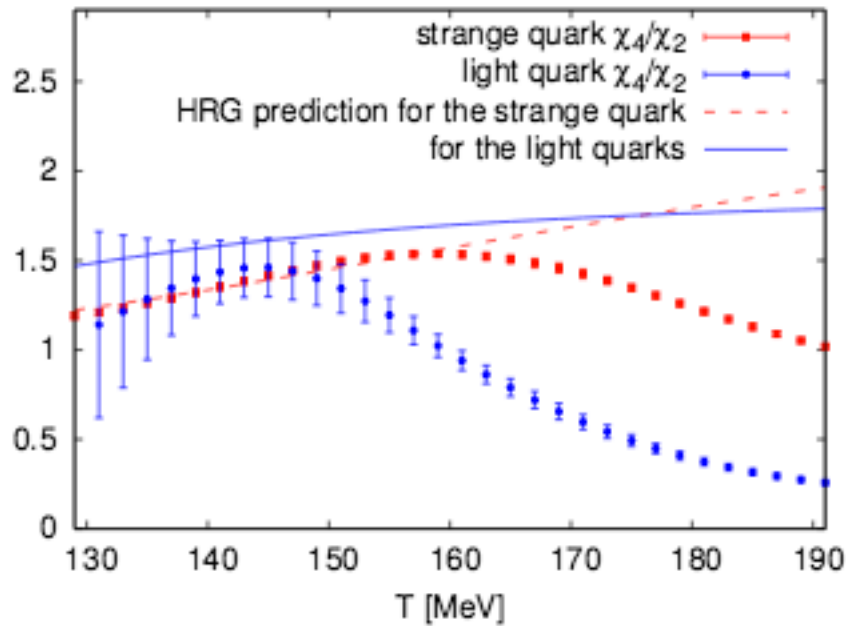
- Rapidity dependence of moments needs to be studied for $1 < \Delta\eta < 2$
- Difference in kinematic cuts between STAR and PHENIX leads to a 5% difference in T_f

Talk by F. Karsch on Monday

Talk by J. Thaefer on Monday

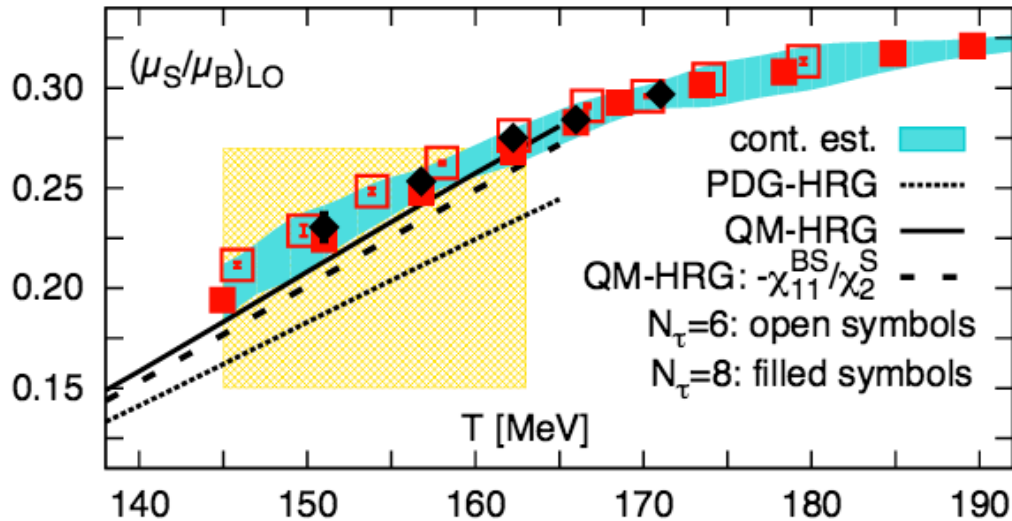
Strangeness fluctuations

WB: R. Bellwied et al, PRL (2013)

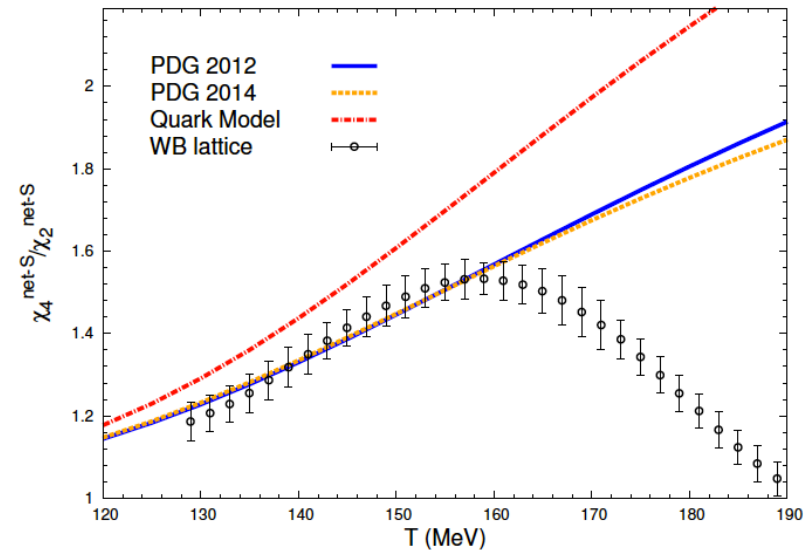


- Lattice data hint at possible flavor-dependence in transition temperature
- Possibility of strange bound-states above T_c ?

Additional strange hadrons



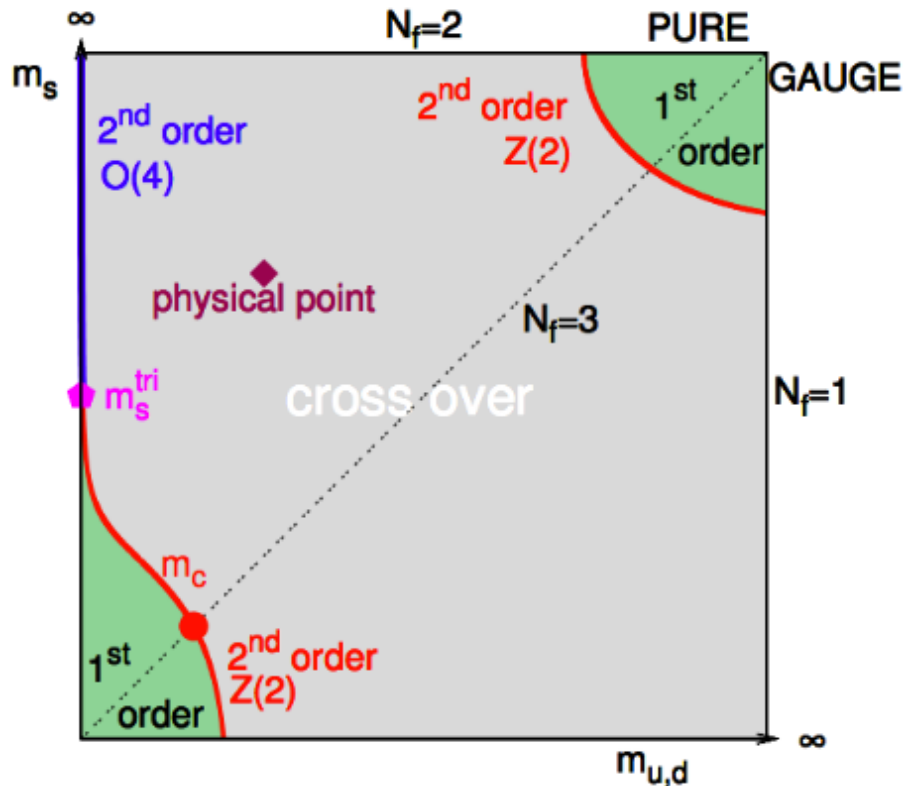
A. Bazavov et al., PRL (2014)



Poster by P. Alba

- Discrepancy between lattice and HRG for μ_S/μ_B can be understood by introducing higher mass states predicted by the Quark Model
- Discrepancy between QM predictions and lattice data for χ_4^S/χ_2^S needs to be understood
- Their effect on freeze-out conditions needs to be investigated taking into account their decay feed-down into stable states

Columbia plot



- Pure gauge theory: $T_c=294(2)$ MeV

Francis et al., 1503.05652

- $N_f=2$ QCD at $m_\pi > m_\pi^{\text{phys}}$:

- $O(a)$ improved Wilson, $N_t=16$

- $m_\pi=295$ MeV $T_c=211(5)$ MeV

- $m_\pi=220$ MeV $T_c=193(7)$ MeV

Brandt et al., 1310.8326

- Twisted-mass QCD

- $m_\pi=333$ MeV $T_c=180(12)$ MeV

Burger et al., 1412.6748

- $N_f=2+1$ $O(a)$ improved Wilson

- Continuum results

Borsanyi et al., 1504.03676

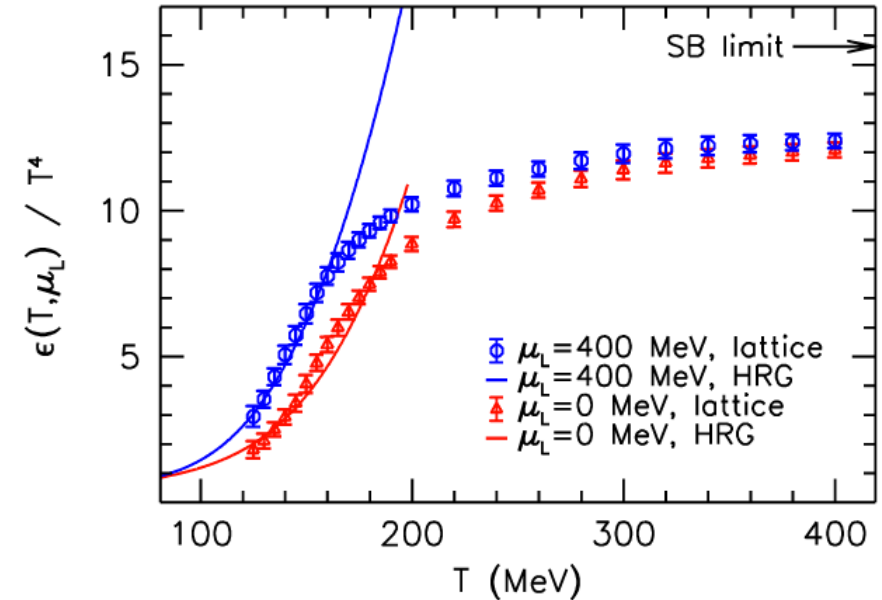
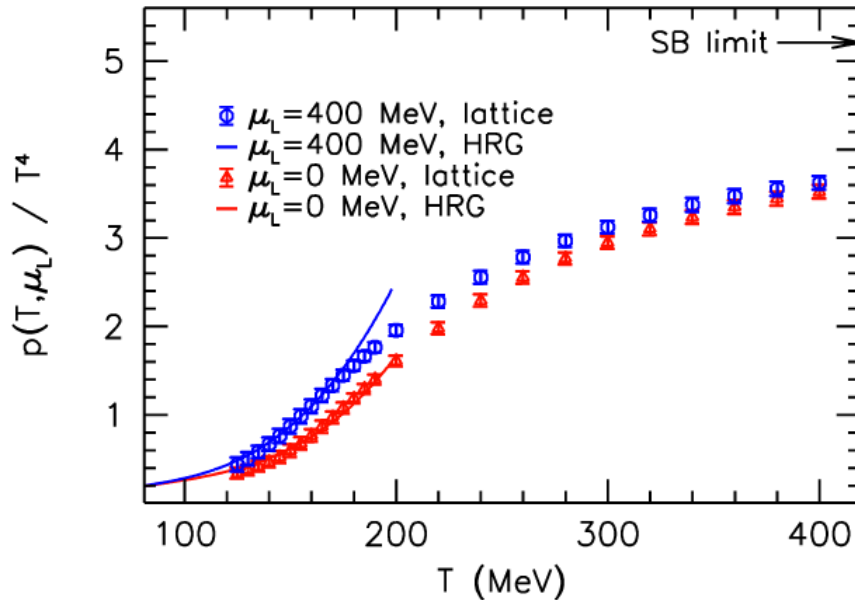
- HISQ action, $N_t=6$, no sign of 1st order phase transition at $m_\pi=80$ MeV

HotQCD, 1312.0119, 1302.5740

Equation of state at $\mu_B > 0$

- Expand the pressure in powers of μ_B (or $\mu_L = 3/2(\mu_u + \mu_d)$)

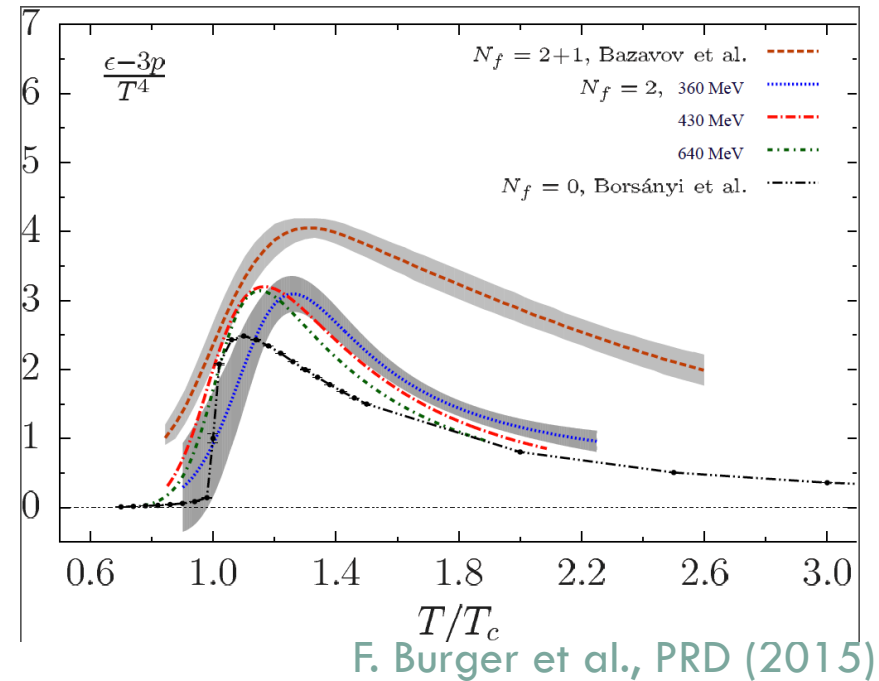
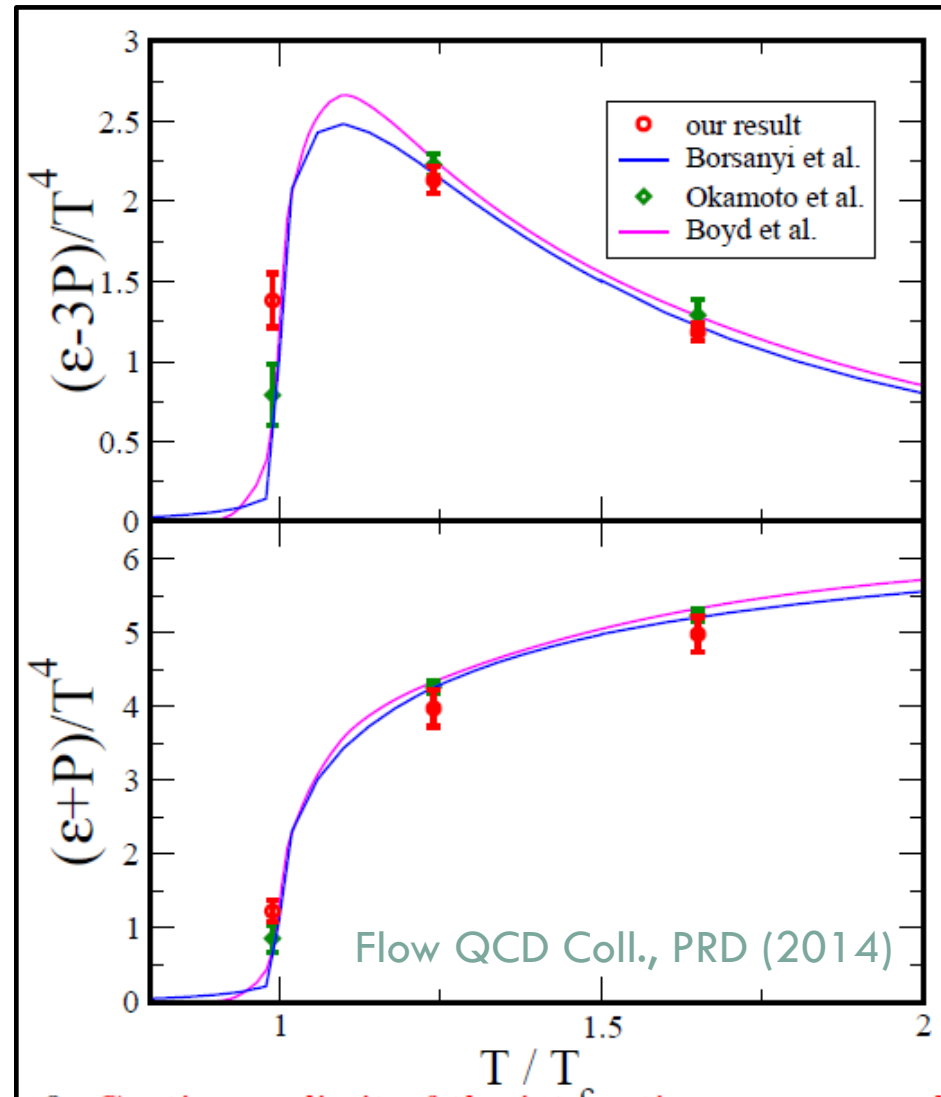
$$\frac{p(T, \{\mu_i\})}{T^4} = \frac{p(T, \{0\})}{T^4} + \frac{1}{2} \sum_{i,j} \frac{\mu_i \mu_j}{T^2} \chi_2^{ij} \quad \text{with} \quad \chi_2^{ij} \equiv \frac{T}{V} \frac{1}{T^2} \frac{\partial^2 \log \mathcal{Z}}{\partial \mu_i \partial \mu_j} \Big|_{\mu_i = \mu_j = 0}$$



S. Borsanyi et al., JHEP (2012)

- Continuum extrapolated results at the physical mass

Alternative methods for thermodynamics



- Gradient flow: EoS in the quenched approximation
- Twisted mass Wilson fermions: EoS available so far for heavier-than-physical quark masses and $N_f=2$